EFFICIENT HERMITE SPECTRAL-GALERKIN METHODS FOR NONLOCAL DIFFUSION EQUATIONS IN UNBOUNDED DOMAINS

HUIYUAN LI†, RUIQING LIU†‡, AND LI-LIAN WANG§

Abstract. In this paper, we develop an efficient Hermite spectral-Galerkin method for nonlocal diffusion equations in unbounded domains. We show that the use of the Hermite basis can de-convolute the troublesome convolutional operations involved in the nonlocal Laplacian. As a result, the "stiffness" matrix can be fast computed and assembled via the four-point stable recursive algorithm with $\mathcal{O}(N^2)$ arithmetic operations. Moreover, the singular factor in a typical kernel function can be fully absorbed by the basis. With the aid of Fourier analysis, we can prove the convergence of the scheme. We demonstrate that the recursive computation of the entries of the stiffness matrix can be extended to the two-dimensional nonlocal Laplacian using the isotropic Hermite functions as basis functions. We provide ample numerical results to illustrate the accuracy and efficiency of the proposed algorithms.

1. Introduction

Mathematical models involving nonlocal operators such as fractional integrals/derivatives, fractional Laplacian and nonlocal Laplacian, have proven to be of great value and superior to conventional models in modeling many abnormal physical phenomena and engineering processes [7, 6]. Although these nonlocal operators are defined in different senses, they have interwoven connections, and share some common numerical difficulties, e.g., the global dependence and the involvement of singular kernels. In general, a nonlocal operator takes the form

$$\mathcal{L}_{\mathcal{K}} u(\boldsymbol{x}) = \text{P.V.} \int_{\mathbb{R}^d} (u(\boldsymbol{x}) - u(\boldsymbol{y}))\mathcal{K}(|\boldsymbol{x}-\boldsymbol{y}|)\mathrm{d}\boldsymbol{y}, \quad \boldsymbol{x} \in \mathbb{R}^d, \tag{1.1}$$

where the kernel $\mathcal{K} : \mathbb{R}^d \to (0, \infty)$ satisfies:

$$\begin{aligned} &\gamma\mathcal{K} \in L^1(\mathbb{R}^d) \ \text{ with } \ \gamma(z) = \min(1, |z|^2), \\ &\exists\, \theta,\, s \in (0,1) \text{ such that } \ \mathcal{K}(\boldsymbol{z}) \ge \theta|\boldsymbol{z}|^{-(d+2s)}, \ \ \boldsymbol{z} \in \mathbb{R}^d \setminus \{0\}. \end{aligned} \tag{1.2}$$

For example, for the hypersingular integral fractional Laplacian $(-\Delta)^s$, we have

$$\mathcal{K}(\eta) = \frac{2^{2s} s\Gamma(s + d/2)}{\pi^{d/2}\Gamma(1-s)} \eta^{-(d+2s)}. \tag{1.3}$$

2000 *Mathematics Subject Classification.* 65N35, 65N25, 33C45, 65M70.

Key words and phrases. nonlocal diffusion equation, spectral-Galerkin, Hermite functions, correlation/convolution, recurrence algorithm.

†State Key Laboratory of Computer Science/Laboratory of Parallel Computing, Institute of Software, Chinese Academy of Sciences, Beijing 100190, China. The research of this authors is supported in part by the National Natural Science Foundation of China (NSFC 11871145 and NSFC 11971016). Email: huiyuan@iscas.ac.cn (H. Li).

‡University of Chinese Academy of Sciences, Beijing 100190, China. Email: ruiqing@iscas.ac.cn (R. Liu).

§Division of Mathematical Sciences, School of Physical and Mathematical Sciences, Nanyang Technological University, 637371, Singapore. The research of this author is partially supported by Singapore MOE AcRF Tier 2 Grants: MOE2018- T2-1-059 and MOE2017-T2-2-144. Email: lilian@ntu.edu.sg (L. Wang).

The second author would like to thank Nanyang Technological University for hosting the visit where this research topic was initialised.

The nonlocal Laplacian operator generally reads

$$\mathcal{L}_\delta[u](\boldsymbol{x}) = \int_{\mathbb{B}_\delta^d} (u(\boldsymbol{x}+\boldsymbol{s}) - u(\boldsymbol{x}))\gamma_\delta(|\boldsymbol{s}|)\mathrm{d}\boldsymbol{s}, \quad \boldsymbol{x} \in \mathbb{R}^d. \tag{1.4}$$

Here, $\gamma_\delta(z)$ is a nonnegative compactly supported kernel whose support is contained in $[0, \delta]$ and $\mathbb{B}_\delta^d$ is a d-dimensional ball of radius δ.

The properties and applications of the nonlocal operator have been extensively investigated. We refer to [9, 8, 7] for a comprehensive exposition of the nonlocal calculus and nonlocal diffusion problems with volume constraints. The δ-compatible studies (i.e., the limit case when $\delta \to 0$) at both continuous and discrete levels were conducted in [30, 29] and some other literature. In fact, when $\delta \to \infty$, it demonstrates that the nonlocal operator can become fractional Laplacian operator in [5]. Many methods and schemes have been exploited to approximate the nonlocal operator, such as domain decomposition method [1], asymptotically compatible schemes [31], discontinuous Galerkin methods [32], and Fourier spectral method [11] among others. Not restricted to these methods, more attempts have been made in studying the solutions of various equations comprising the nonlocal operator, including nonlocal equations with Dirichlet boundaries [14], nonlocal wave equations [3] and nonlocal Allen-Cahn type equations [4].

While most existing works are on the nonlocal problems in bounded domains (and many are for one spatial dimension), there has been much less concern about nonlocal models in the unbounded domain, where such nonlocal operators are naturally set without complications from the boundary. It is noteworthy that a nonlocal diffusion equation on the real line is considered in [36], where the infinite interval was reduced to a finite one by an artificial layer based on the z-transform. The study of the nonlocal analogue of artificial boundary conditions/layers is also a subject of interest [35, 10, 12], but the rigorous error analysis and many other aspects are still worthy of deeper investigation.

In this paper, we propose an efficient and accurate spectral method to directly solve nonlocal equations in $\mathbb{R}^d$ with $d = 1, 2$, though the essential idea can be extended to $d = 3$ (but it is more involved). To fix the idea, we consider the model equation:

$$-\mathscr{L}_\delta u(x) + \lambda u(x) = f(x), \quad x \in \mathbb{R}; \quad \lim_{|x|\to\infty} u(x) = 0, \tag{1.5}$$

where $\lambda > 0$, and the nonlocal operator is defined as

$$\mathscr{L}_\delta u(x) = \int_{-\delta}^{\delta} (u(x+s) - u(x))\gamma_\delta(|s|)\mathrm{d}s, \tag{1.6}$$

with $\gamma_\delta(\cdot)$ being a non-negative and radial nonlocal kernel such that

$$\gamma_\delta(s) = \frac{\omega_\delta(s)}{s^2}, \quad 0 < \omega_\delta(s) \le \frac{C_\delta}{s^\mu}, \quad s \in (0, \delta),\ \mu \in [0, 1), \tag{1.7}$$

for some positive constant $C_\delta > 0$. We find readily that

$$-\int_{-\infty}^{\infty} \mathscr{L}_\delta u(x)v(x)\mathrm{d}x = \int_0^\delta \left[\int_{-\infty}^{\infty} (u(x+s) - u(x))(v(x+s) - v(x))\mathrm{d}x\right]\gamma_\delta(s)\mathrm{d}s := \mathbb{B}_\delta(u, v).$$

It is seen that the main difficulty lies in the convolution and the singular kernel. The key to the efficiency of the algorithm to be developed resides in that (i) the Hermite basis can analytically de-convolute the inner integral, and the entries of the stiffness matrix can be computed by some recursive formulas; and (ii) the typical singularity of the kernel can be absorbed in the computation. Accordingly, the cost for evaluating the stiffness matrix amounts to $\mathcal{O}(N^2)$. As we shall see in both algorithm development and error analysis, the appealing property of the Hermite functions under the Fourier transform becomes an important piece of the puzzle. We remark that there has been much recent interest in Hermite spectral methods for PDEs involving usual or integral fractional Laplacian in unbounded domains [2, 23, 24, 27, 34, 26] (also see [25, 28] for rational approximation). However, it is unknown if the Hermite method is equally or more efficient for the nonlocal Laplacian. In what follows, we aim at giving an affirmative answer to this.

The rest of the paper is organised as follows. In Section 2, we collect some relevant properties of Hermite and Laguerre functions, which are important for the development of efficient spectral algorithms. In Section 3, we present the Hermite spectral-Galerkin approximation scheme with a detailed implementation and rigorous error analysis in one dimension. In Section 4, we provide ample numerical results to show the accuracy and efficiency of the proposed method. In Section 5, we extend the algorithm to two-dimensional setting and validate the recursive formula for the computation of the entries of the stiffness matrix.

2. Properties of Hermite and Laguerre functions

We present some important formulas of Hermite functions together with the closely connected Laguerre polynomials that are crucial for the construction of efficient spectral algorithm. Throughout this paper, we denote by $\mathbb{R}$, $\mathbb{Z}$, $\mathbb{N}_0$ and $\mathbb{Z}^-$ the set of real numbers, integers, nonnegative integers and negative integers, respectively. We also denote by $\lfloor a \rfloor$ the largest integer $\le a$, and by a^- the negative part of a, .i.e., $a^- = \max(-a, 0)$.

2.1. **Hermite polynomials/functions.**

We review some properties of the Hermite polynomials, which can be found from various resources (see, e.g., [16, 22]). The Hermite polynomials $H_n(x)$, $n \in \mathbb{N}_0$, defined on $\mathbb{R} := (-\infty, \infty)$, are orthogonal with respect to the Hermite weight function $\omega(x) = \mathrm{e}^{-x^2}$, namely,

$$\int_{-\infty}^{\infty} H_m(x)\, H_n(x)\, \omega(x)\, \mathrm{d}x = h_n \delta_{mn}, \quad h_n := \sqrt{\pi}\, 2^n n!, \quad m, n \in \mathbb{N}_0. \tag{2.1}$$

The Hermite polynomials satisfy the three-term recurrence relation:

$$H_{n+1}(x) = 2xH_n(x) - 2nH_{n-1}(x), \quad n \ge 1, \quad H_0(x) = 1, \quad H_1(x) = 2x. \tag{2.2}$$

Note that $H_n(x)$ is odd (resp. even) for n odd (resp. even), and we have

$$H_n(-x) = (-1)^n H_n(x); \quad H_{2n+1}(0) = 0, \quad H_{2n}(0) = (-1)^n \frac{(2n)!}{n!}. \tag{2.3}$$

The Hermite polynomials satisfy the derivative relation:

$$\partial_x^k H_n(x) = \frac{2^k n!}{(n-k)!} H_{n-k}(x), \quad n \ge k \ge 1, \tag{2.4}$$

where we denoted the usual derivatives by $\partial_x^k = \frac{d^k}{dx^k}$. It is important to point out that the polynomial $H_n(x)$ grows exponentially with respect to x with the upper bound (cf. [22]):

$$|H_n(x)| < c 2^{n/2} \sqrt{n!}\, \mathrm{e}^{x^2/2}, \quad c \approx 1.086435. \tag{2.5}$$

Moreover, it has the asymptotic behaviour for large n and fixed x on any finite interval (cf. [15]):

$$\begin{aligned} \frac{\Gamma(n/2+1)}{n!} \mathrm{e}^{-x^2/2} H_n(x) &= \cos\big(\sqrt{2n+1}\, x - n\pi/2\big) \\ &\quad + \frac{x^3}{6\sqrt{2n+1}} \sin\big(\sqrt{2n+1}\, x - n\pi/2\big) + O(n^{-1}). \end{aligned} \tag{2.6}$$

The exponential growth of Hermite polynomials causes severe numerical instability, and makes the basis unsuitable for approximating functions with decay at infinity.

In practice, we employ the Hermite functions with a tunable scaling parameter $\alpha > 0$,

$$\widehat{H}_n^{(\alpha)}(x) = \sqrt{\frac{\alpha}{h_n}}\, \mathrm{e}^{-\alpha^2 x^2/2} H_n(\alpha x), \quad x \in \mathbb{R}. \tag{2.7}$$

By (2.1), they are mutually orthogonal, i.e.,

$$\int_{-\infty}^{\infty} \widehat{H}_n^{(\alpha)}(x) \widehat{H}_m^{(\alpha)}(x)\, \mathrm{d}x = \delta_{mn}. \tag{2.8}$$

The Fourier transform of the Hermite function is still a Hermite function but with a different scaling factor.

Lemma 2.1. *We have the explicit formula for the Fourier transform of the Hermite functions:*

$$\mathscr{F}[\widehat{H}_n^{(\alpha)}](\xi) = \int_{-\infty}^{\infty} \widehat{H}_n^{(\alpha)}(x) \mathrm{e}^{-\mathrm{i}\xi x} \mathrm{d}x = (-\mathrm{i})^n \sqrt{2\pi}\, \widehat{H}_n^{(1/\alpha)}(\xi). \tag{2.9}$$

Proof. Using the integral formula of the Hermite polynomials (cf. [17, 7.376]):

$$\int_{-\infty}^{\infty} \mathrm{e}^{\mathrm{i}xy} H_n(x)\, \mathrm{e}^{-x^2/2}\, \mathrm{d}x = \sqrt{2\pi}\, \mathrm{i}^n \mathrm{e}^{-y^2/2}\, H_n(y), \tag{2.10}$$

and the variable substitutions: $x = \alpha t$ and $y = -\xi/\alpha$, we can obtain (2.9) from (2.3), (2.7) and the above identity immediately. □

The convolution of two functions is defined by

$$(f * g)(x) = \int_{-\infty}^{\infty} f(y) g(x-y)\, \mathrm{d}y.$$

Using Lemma 2.1, we can derive the following convolution property, which is of paramount importance for the spectral algorithm to be developed.

Theorem 2.1. *For $\alpha > 0$, we have*

$$\big[\widehat{H}_n^{(\alpha)} * \widehat{H}_m^{(\alpha)}\big](x) = Y_{m,n}^{(\alpha)}(x) := \sum_{l=0}^{\min(m,n)} \frac{(-1)^l\, 2^l\, l!}{\sqrt{2^{m+n}\, m!\, n!}} \binom{m}{l} \binom{n}{l} (\alpha x)^{m+n-2l} \mathrm{e}^{-(\alpha x)^2/4}. \tag{2.11}$$

Proof. Using the convolution property of Fourier transform and the formula (2.9), we find

$$\mathscr{F}[\widehat{H}_m^{(\alpha)} * \widehat{H}_n^{(\alpha)}] = \mathscr{F}[\widehat{H}_m^{(\alpha)}] \times \mathscr{F}[\widehat{H}_n^{(\alpha)}] = 2(-\mathrm{i})^{m+n} \pi \widehat{H}_m^{(1/\alpha)}(\xi)\, \widehat{H}_n^{(1/\alpha)}(\xi). \tag{2.12}$$

Using the product formula of Hermite polynomials (cf. [15]):

$$H_n(\xi)\, H_m(\xi) = \sum_{l=0}^{\min(m,n)} \binom{m}{l} \binom{n}{l} 2^l l!\, H_{m+n-2l}(\xi), \tag{2.13}$$

we obtain from (2.7) that

$$\widehat{H}_m^{(1/\alpha)}(\xi)\, \widehat{H}_n^{(1/\alpha)}(\xi) = \sum_{l=0}^{\min(m,n)} \sqrt{\frac{h_{m+n-2l}}{\alpha h_m h_n}} \binom{m}{l} \binom{n}{l} 2^l l!\, \mathrm{e}^{-\xi^2/(2\alpha^2)}\, \widehat{H}_{m+n-2l}^{(1/\alpha)}(\xi). \tag{2.14}$$

Recall the identity of the Hermite polynomials (cf. [15, 18.18.23]):

$$\int_{-\infty}^{\infty} \mathrm{e}^{-xz} H_n(x)\, \mathrm{e}^{-x^2}\, \mathrm{d}x = \sqrt{\pi}\, (-z)^n\, \mathrm{e}^{z^2/4}, \tag{2.15}$$

for any complex z. Consequently, we find the inverse Fourier transform:

$$
\begin{aligned}
\mathscr{F}^{-1}\big[\mathrm{e}^{-\xi^2/(2\alpha^2)}\,\widehat{H}^{(1/\alpha)}_{m+n-2l}(\xi)\big](x) &= \frac{1}{2\pi}\int_{-\infty}^{\infty} \mathrm{e}^{\mathrm{i}\xi x}\mathrm{e}^{-\xi^2/(2\alpha^2)}\,\widehat{H}^{(1/\alpha)}_{m+n-2l}(\xi)\,\mathrm{d}\xi \\
&= \frac{1}{2\pi}\frac{1}{\sqrt{\alpha h_{m+n-2l}}}\int_{-\infty}^{\infty} \mathrm{e}^{\mathrm{i}\xi x}\mathrm{e}^{-\xi^2/\alpha^2}\,H_{m+n-2l}(\xi/\alpha)\,\mathrm{d}\xi \\
&= \frac{1}{2\pi}\frac{\sqrt{\alpha}}{\sqrt{h_{m+n-2l}}}\int_{-\infty}^{\infty} \mathrm{e}^{\mathrm{i}\alpha\xi x}\,H_{m+n-2l}(\xi)\,\mathrm{e}^{-\xi^2}\mathrm{d}\xi \\
&= \frac{\sqrt{\alpha}\,\mathrm{i}^{m+n-2l}}{2\sqrt{\pi h_{m+n-2l}}}(\alpha x)^{m+n-2l}\mathrm{e}^{-(\alpha x)^2/4}.
\end{aligned} \tag{2.16}
$$

Applying the inverse Fourier transform to both sides of (2.12), we deduce from (2.14)-(2.16) that

$$
(\widehat{H}^{(\alpha)}_m * \widehat{H}^{(\alpha)}_n)(x) = \sum_{l=0}^{\min(m,n)} \frac{\sqrt{\pi}(-1)^l 2^l l!}{\sqrt{h_m h_n}}\binom{m}{l}\binom{n}{l}(\alpha x)^{m+n-2l}\mathrm{e}^{-(\alpha x)^2/4}. \tag{2.17}
$$

Then we obtain (2.11) directly by substituting the constants h_m and h_n into (2.17). ☐

2.2. **Generalized Laguerre polynomials.** Now we introduce generalized Laguerre polynomials and explore their connections with Hermite polynomials/functions. Let us first recall the definition of classic Laguerre polynomials for $\mu > -1$,

$$
\mathcal{L}^\mu_k(x) = \sum_{\nu=0}^{k} \frac{(\mu+\nu+1)_{k-\nu}}{(k-\nu)!\nu!}(-x)^\nu, \qquad k = 0, 1, \ldots \tag{2.18}
$$

This explicit representation furnishes the extension of $\mathcal{L}^\mu_k(x)$ to arbitrary $\mu \in \mathbb{R}$, which are referred to as the generalized Laguerre polynomials (cf. [21]). Specifically, we have

$$
\mathcal{L}^\mu_0(x) = 1, \qquad \mathcal{L}^\mu_1(x) = \mu + 1 - x.
$$

Generalized Laguerre polynomials possess the following recurrence relations,

$$
\mathcal{L}^\mu_n(x) = \mathcal{L}^{\mu+1}_n(x) - \mathcal{L}^{\mu+1}_{n-1}(x), \tag{2.19}
$$

$$
x\mathcal{L}^\mu_n(x) = (n+\mu)\mathcal{L}^{\mu-1}_n(x) - (n+1)\mathcal{L}^{\mu-1}_{n+1}(x) \tag{2.20}
$$

$$
= -(n+\mu)\mathcal{L}^\mu_{n-1}(x) + (2n+\mu+1)\mathcal{L}^\mu_n(x) - (n+1)\mathcal{L}^\mu_{n+1}(x). \tag{2.21}
$$

Moreover, generalized Laguerre polynomials for $\mu \in \mathbb{Z}^- \cup (-1, \infty)$ are orthogonal to each other with respect to the weight function $\mathrm{e}^{-x}x^\mu$,

$$
\int_0^\infty \mathcal{L}^\mu_k(x)\mathcal{L}^\mu_j(x)\mathrm{e}^{-x}x^\mu dx = \frac{\Gamma(k+\mu+1)}{k!}\delta_{j,k}, \qquad j, k \geq \lfloor \mu^- \rfloor. \tag{2.22}
$$

Besides, the flection property holds for any $\mu \in \mathbb{Z}$,

$$
\mathcal{L}^\mu_k(x) = (-x)^{-\mu}\frac{\Gamma(k+\mu+1)}{k!}\mathcal{L}^{-\mu}_{k+\mu}(x), \qquad k \geq \mu^-; \tag{2.23}
$$

Generalized Laguerre polynomials and Hermite polynomials/functions are closely connected. On the one hand, Hermite polynomials can be entirely reduced to Laguerre polynomials,

$$
H_{2k+\mu}(x) = (-1)^k 2^{2k+\mu} m! x^\mu \mathcal{L}^{\mu-\frac{1}{2}}_k(x^2), \qquad k \geq 0,\ \mu = 0, 1.
$$

One the other hand, the following lemma states that the convolution of two Hermite functions in Theorem 2.1 is actually a generalized Hermite function which can be represented by generalized Laguerre polynomials.

Lemma 2.2. *It holds that*

$$
\begin{aligned}
Y^{(\alpha)}_{m,n}(x) &= (-1)^m\sqrt{\frac{m!}{n!}}\left(\frac{\alpha x}{\sqrt{2}}\right)^{n-m} \mathrm{e}^{-\frac{(\alpha x)^2}{4}}\mathcal{L}^{n-m}_m\left(\frac{(\alpha x)^2}{2}\right) \\
&= \begin{cases} (-1)^m\sqrt{\frac{m!}{n!}}\left(\frac{\alpha x}{\sqrt{2}}\right)^{n-m} \mathrm{e}^{-\frac{(\alpha x)^2}{4}}\mathcal{L}^{n-m}_m\left(\frac{(\alpha x)^2}{2}\right), & n\ge m, \\ (-1)^n\sqrt{\frac{n!}{m!}}\left(\frac{\alpha x}{\sqrt{2}}\right)^{m-n} \mathrm{e}^{-\frac{(\alpha x)^2}{4}}\mathcal{L}^{m-n}_n\left(\frac{(\alpha x)^2}{2}\right), & m\ge n. \end{cases}
\end{aligned} \tag{2.24}
$$

Proof. Indeed, one readily derives (2.24) from (2.11), (2.18) and (2.23). □

Remark 2.1. Similar results are established by Lasser et al. for the Wigner transform of Hermite functions [20].

3. Hermite spectral-Galerkin method: implementation and error analysis

In this section, we introduce an efficient spectral-Galerkin method for PDEs with nonlocal operators and then give some details on its implementation.

We consider the problem (1.5). Define the energy space as

$$
\mathcal{H}^1_\delta(\mathbb{R}) := \Big\{u\in L^2(\mathbb{R})\,:\, \int_{-\infty}^{\infty}\int_{-\delta}^{\delta}\big(u(x+s)-u(x)\big)^2\gamma_\delta(|s|)\,\mathrm{d}s\mathrm{d}x<\infty\Big\}, \tag{3.1}
$$

which is equipped with the semi-norm

$$
|u|_{\mathcal{H}^1_\delta} = \Big\{\frac{1}{2}\int_{-\infty}^{\infty}\int_{-\delta}^{\delta}|u(x+s)-u(x)|^2\gamma_\delta(|s|)\,\mathrm{d}s\mathrm{d}x\Big\}^{1/2}, \tag{3.2}
$$

and the norm

$$
\|u\|_{\mathcal{H}^1_\delta} = \big(|u|^2_{\mathcal{H}^1_\delta}+\|u\|^2\big)^{1/2}, \qquad \|u\|^2=\int_{-\infty}^{\infty}|u(x)|^2\,\mathrm{d}x. \tag{3.3}
$$

Further introduce the bilinear form

$$
\begin{aligned}
\mathbb{B}_\delta(u,v) = {}& \frac{1}{2}\int_{-\infty}^{\infty}\int_{-\delta}^{\delta}\big(u(x+s)-u(x)\big)\big(v(x+s)-v(x)\big)\gamma_\delta(|s|)\,\mathrm{d}s\mathrm{d}x \\
&+\lambda\int_{-\infty}^{\infty}u(x)v(x)\,\mathrm{d}x, \quad \forall\, u,v\in\mathcal{H}^1_\delta(\mathbb{R}).
\end{aligned} \tag{3.4}
$$

Then a weak form of (1.5) reads: to find $u\in\mathcal{H}^1_\delta(\mathbb{R})$ such that

$$
\mathbb{B}_\delta(u,v)=(f,v), \quad \forall\, v\in\mathcal{H}^1_\delta(\mathbb{R}). \tag{3.5}
$$

The Hermite spectral-Galerkin scheme for (1.5) is to find

$$
u_N\in\mathcal{V}_N := \mathrm{span}\big\{\widehat{H}^{(\alpha)}_n\,:\,0\le n\le N\big\}, \tag{3.6}
$$

such that

$$
\mathbb{B}_\delta(u_N,\psi)=(\widehat{I}_N f,\psi), \quad \forall\,\psi\in\mathcal{V}_N, \tag{3.7}
$$

where $\widehat{I}_N f\in\mathcal{V}_N$ is the Lagrange interpolation associated with the Hermite functions at $N+1$ Hermite-Gauss points (cf. [18]), i.e.,

$$
\big[\widehat{I}_N f\big]\Big(\frac{x^{(N)}_k}{\alpha}\Big) = f\Big(\frac{x^{(N)}_k}{\alpha}\Big), \qquad k=0,1,\dots,N,
$$

with $x^{(N)}_0<x^{(N)}_1<\cdots<x^{(N)}_N$ being the zeros of the Hermite polynomial $H_{N+1}(x)$. It is evident that by the Lax-Milgram Lemma, both (3.5) and (3.7) admit a unique solution for any fixed $\delta>0$.

3.1. **Implementation.** To form the matrix form of (3.7), we write $u_N(x) = \sum_{n=0}^N \hat{u}_n \widehat{H}_n^{(\alpha)}(x)$, and denote

$$\hat{\boldsymbol{u}} = (\hat{u}_0, \hat{u}_1, \cdots, \hat{u}_N)^{\rm t}, \quad \boldsymbol{f} = (f_0, f_1, \cdots, f_N)^{\rm t}, \quad f_n = (\widehat{I}_N f, \widehat{H}_n^{(\alpha)}), \tag{3.8}$$

so the linear system of (3.7) takes the form

$$\big(\boldsymbol{S} + \lambda \boldsymbol{I}\big)\hat{\boldsymbol{u}} = \boldsymbol{f}, \tag{3.9}$$

where the mass matrix is identity due to the orthogonality (2.8). We now compute the stiffness matrix

$$\boldsymbol{S}_{m,n} = \int_0^\delta \varPhi_{m,n}^{(\alpha)}(s)\gamma_\delta(s)\,{\rm d}s, \tag{3.10}$$

where

$$\begin{aligned}\varPhi_{m,n}^{(\alpha)}(s) &:= \int_{-\infty}^{\infty} (\widehat{H}_n^{(\alpha)}(x+s) - \widehat{H}_n^{(\alpha)}(x))(\widehat{H}_m^{(\alpha)}(x+s) - \widehat{H}_m^{(\alpha)}(x))\,{\rm d}x \\ &= 2\int_{-\infty}^{\infty} \widehat{H}_n^{(\alpha)}(x)\widehat{H}_m^{(\alpha)}(x){\rm d}x - \int_{-\infty}^{\infty} \widehat{H}_n^{(\alpha)}(x+s)\widehat{H}_m^{(\alpha)}(x)\,{\rm d}x - \int_{-\infty}^{\infty} \widehat{H}_n^{(\alpha)}(x)\widehat{H}_m^{(\alpha)}(x+s)\,{\rm d}x.\end{aligned} \tag{3.11}$$

We infer from (2.3) and (2.11) that

$$\int_{-\infty}^{\infty} \widehat{H}_m^{(\alpha)}(x)\widehat{H}_n^{(\alpha)}(s+x)\,{\rm d}x = (-1)^m Y_{m,n}^{(\alpha)}(s) = (-1)^m Y_{n,m}^{(\alpha)}(s). \tag{3.12}$$

Thus, by (2.8), (3.11) and (3.12),

$$\varPhi_{m,n}^{(\alpha)}(s) = 2\delta_{mn} - \big[(-1)^m + (-1)^n\big]\, Y_{m,n}^{(\alpha)}(s), \quad s \in (0, \delta), \tag{3.13}$$

which implies $\varPhi_{m,n}^{(\alpha)}$ is symmetric with respect to m and n, and $\varPhi_{m,n}^{(\alpha)}(s) = 0$ if $m+n$ is odd.

Lemma 3.1. *$\varPhi_{m,n}^{(\alpha)}$ in (3.11) with even $m+n$ satisfy the recurrence relation:*

$$\varPhi_{n,n}^{(\alpha)}(s) = 2 - 2\,{\rm e}^{-\frac{(\alpha s)^2}{4}} \mathcal{L}_n^0\big(\tfrac{\alpha^2 s^2}{2}\big), \qquad n = 0, 1\ldots, \tag{3.14}$$

$$\sqrt{n+1}\,\varPhi_{m+1,n+1}^{(\alpha)}(s) = \sqrt{m+1}\,\varPhi_{m,n}^{(\alpha)}(s) + \sqrt{n}\,\varPhi_{m+1,n-1}^{(\alpha)}(s) - \sqrt{m+2}\,\varPhi_{m+2,n}^{(\alpha)}(s). \tag{3.15}$$

Proof. It suffices to prove that $Y_{m,n}^{(\alpha)}$, $m \ge n \ge 0$, satisfy the following recurrence relation,

$$\sqrt{m+2}\,Y_{m+2,n}^{(\alpha)}(s) + \sqrt{n}\,Y_{m+1,n-1}^{(\alpha)}(s) = \sqrt{n+1}\,Y_{m+1,n+1}^{(\alpha)}(s) + \sqrt{m+1}\,Y_{m,n}^{(\alpha)}(s), \tag{3.16}$$

$$Y_{n,n}^{(\alpha)}(s) = (-1)^n\,{\rm e}^{-\frac{(\alpha s)^2}{4}}\,\mathcal{L}_n^0\big(\tfrac{\alpha^2 s^2}{2}\big). \tag{3.17}$$

Indeed, one verifies readily that

$$\begin{aligned} l!\left[\binom{m+2}{l}\binom{n}{l} - \binom{m+1}{l}\binom{n+1}{l}\right] &= \frac{(n-m-1)(m+1)!n!}{(l-1)!(m+2-l)!(n+1-l)!} \\ = -\,(l-1)!\left[(m+1)\binom{m}{l-1}\binom{n}{l-1} - n\binom{m+1}{l-1}\binom{n-1}{l-1}\right]. \end{aligned}$$

Multiplying both sides of the above identity by $\frac{(-1)^l 2^l {\rm e}^{-\frac{(\alpha x)^2}{4}}(\alpha s)^{m+n+2-2l}}{\sqrt{2^{m+n+2}(m+1)!n!}}$ and summing them up with respect to l, one finds that

$${\rm e}^{-\frac{(\alpha s)^2}{4}} \sum_{l=0}^{\infty} \frac{(-1)^l 2^l l! \sqrt{m+2}}{\sqrt{2^{m+2+n}(m+2)!n!}}\binom{m+2}{l}\binom{n}{l}(\alpha s)^{m+2+n-2l}$$

$$
\begin{aligned}
&- \mathrm{e}^{-\frac{(\alpha s)^2}{4}} \sum_{l=0}^{\infty} \frac{(-1)^l 2^l l! \sqrt{n+1}}{\sqrt{2^{m+1+n+1}(m+1)!(n+1)!}} \binom{m+1}{l} \binom{n+1}{l} (\alpha s)^{m+1+n+1-2l} \\
=&\mathrm{e}^{-\frac{(\alpha s)^2}{4}} \sum_{l=0}^{\infty} \frac{(-1)^{l-1} 2^{l-1} (l-1)! \sqrt{m+1}}{\sqrt{2^{m+n} m! n!}} \binom{m}{l-1} \binom{n}{l-1} (\alpha s)^{m+n+2-2l} \\
&- \mathrm{e}^{-\frac{(\alpha s)^2}{4}} \sum_{l=0}^{\infty} \frac{(-1)^{l-1} 2^{l-1} (l-1)! \sqrt{n}}{\sqrt{2^{m+n}(m+1)!(n-1)!}} \binom{m+1}{l-1} \binom{n-1}{l-1} (\alpha s)^{m+n+2-2l}.
\end{aligned}
$$

From the definition of $Y_{m,n}^{(\alpha)}$, we can rewrite the above as

$$
\sqrt{m+2}\, Y_{m+2,n}^{(\alpha)}(s) - \sqrt{n+1}\, Y_{m+1,n+1}^{(\alpha)}(s) = \sqrt{m+1}\, Y_{m,n}^{(\alpha)}(s) - \sqrt{n}\, Y_{m+1,n-1}^{(\alpha)}(s),
$$

which gives (3.16).

Noting that (3.17) is an immediate consequence of (2.24), we complete the proof. □

With the above preparations, we can calculate the entries of the stiffness matrix. Also we note that $\boldsymbol{S}$ is symmetric. Thus, it suffices to compute the entries $\boldsymbol{S}_{m+n,n}$ with nonnegative even m. Below we state our main result as a direct consequence of Lemma 3.1.

Theorem 3.1. *$\boldsymbol{S}_{m+n,n} = 0$ if m is odd. Otherwise, we have the following recurrence algorithm for even $m \geq 0$,*

$$
\begin{aligned}
\boldsymbol{S}_{m+n,n} = \sqrt{\frac{m+n-1}{m+n}}\, \boldsymbol{S}_{m+n-2,n} + \sqrt{\frac{n}{m+n}}\, \boldsymbol{S}_{m+n-1,n-1} - \sqrt{\frac{n+1}{m+n}}\, \boldsymbol{S}_{m+n-1,n+1}, \\
n = 0, 1, \ldots, \quad m = 2, 4, \ldots,
\end{aligned}
\tag{3.18}
$$

with the initial conditions

$$
\boldsymbol{S}_{n,n} = 2 \int_0^{\delta} \Big[1 - \mathrm{e}^{-\frac{(\alpha s)^2}{4}} \mathcal{L}_n^0\big(\tfrac{\alpha^2 s^2}{2}\big)\Big] \gamma_\delta(s)\, \mathrm{d}s, \quad n = 0, 1, \ldots. \tag{3.19}
$$

Typically, we consider in this paper the kernel function:

$$
\gamma_\delta(s) = \frac{\omega_\delta(s)}{s^2}, \quad \omega_\delta(s) \leq \frac{C_\delta}{s^\mu}, \tag{3.20}
$$

for $\mu \in [0,1),\ s \in (0,\delta)$ and some positive constant $C_\delta > 0$. Note that the singular factor s^{-2} can be absorbed in (3.19) by $1 - \mathrm{e}^{-\frac{(\alpha s)^2}{4}} \mathcal{L}_n^0\big(\frac{\alpha^2 s^2}{2}\big)$ owing to the fact that $\mathcal{L}_n^0(0) = 1$. Hence $\boldsymbol{S}_{n,n}$ can be computed accurately by using a Jacobi-Gauss quadrature with respect to the weight $s^{-\mu}$ with $\mu \in [0,1)$.

3.2. **Error analysis.** For clarity of presentation, we shall drop the scaling parameters in the description of error analysis, and simply denote $\widehat{H}_n(x) = \widehat{H}_n^{(1)}(x)$.

As with the error analysis of the (local) elliptic problems, it is essential to consider H_δ^1-orthogonal projection under the inner product of the space defined in (3.1). More precisely, we define the orthogonal projection $\widehat{\Pi}_N^\delta : \mathcal{H}_\delta^1(\mathbb{R}) \to \mathcal{V}_N$ such that

$$
\big(u - \widehat{\Pi}_N^\delta u, v_N\big)_{\mathcal{H}_\delta^1} = 0, \quad \forall\, v_N \in \mathcal{V}_N, \tag{3.21}
$$

where the H_δ^1-inner product is given by

$$
\begin{aligned}
(u,v)_{\mathcal{H}_\delta^1} =& \frac{1}{2} \int_{-\infty}^{\infty} \int_{-\delta}^{\delta} (u(x+s) - u(x))(v(x+s) - v(x)) \gamma_\delta(|s|)\, \mathrm{d}s \mathrm{d}x \\
&+ \int_{-\infty}^{\infty} u(x) v(x)\, \mathrm{d}x, \quad \forall\, u, v \in \mathcal{H}_\delta^1(\mathbb{R}).
\end{aligned}
\tag{3.22}
$$

By the projection theorem, we have

$$\|u-\widehat{\varPi}_N^{\delta}u\|_{\mathcal{H}_\delta^1}=\inf_{\varPsi\in\mathcal{V}_N}\|u-\varPsi\|_{\mathcal{H}_\delta^1}. \tag{3.23}$$

The following bound plays an important part in the error analysis.

Lemma 3.2. *Let $\gamma_\delta(s)$ be a general kernel function such that*

$$\gamma_\delta(s)=\frac{\omega_\delta(s)}{s^2},\quad \omega_\delta(s)\le\frac{C_\delta}{s^\mu},\quad \mu\in[0,1),\;\; s\in(0,\delta),\;\; \delta>0. \tag{3.24}$$

Then for any $u\in H_\delta^1(\mathbb{R})$, we have

$$|u|_{\mathcal{H}_\delta^1}\le D_{\delta,\mu}\|u'\|,\quad \textit{where}\quad D_{\delta,\mu}:=\sqrt{\frac{2C_\delta\delta^{1-\mu}}{1-\mu}}. \tag{3.25}$$

Proof. By the definition (3.2),

$$|u|^2_{\mathcal{H}_\delta^1}=\int_{-\delta}^{\delta}\varPhi(s)\gamma_\delta(|s|)\,\mathrm{d}s=2\int_0^{\delta}\varPhi(s)\gamma_\delta(s)\,\mathrm{d}s, \tag{3.26}$$

where

$$\varPhi(s):=\int_{-\infty}^{\infty}\big(u(x+s)-u(x)\big)^2\,\mathrm{d}x. \tag{3.27}$$

Using the Parseval's identity, we find

$$\varPhi(s)=\int_{-\infty}^{\infty}\big(u(x+s)-u(x)\big)^2\,\mathrm{d}x=\frac{1}{2\pi}\int_{-\infty}^{\infty}\big|\mathscr{F}[u(x+s)-u(x)](\xi)\big|^2\,\mathrm{d}\xi. \tag{3.28}$$

By the transition property of the Fourier transform: $\mathscr{F}[u](\xi+s)=\mathrm{e}^{\mathrm{i}\xi s}\mathscr{F}[u](\xi)$, we further obtain

$$\varPhi(s)=\frac{1}{2\pi}\int_{-\infty}^{\infty}\big|(\mathrm{e}^{\mathrm{i}\xi s}-1)\mathscr{F}[u](\xi)\big|^2\,\mathrm{d}\xi=\frac{1}{\pi}\int_{-\infty}^{\infty}\big(1-\cos\xi s\big)\big|\mathscr{F}[u](\xi)\big|^2\,\mathrm{d}\xi. \tag{3.29}$$

Substituting (3.29) into (3.26) and changing order of integration, leads to

$$|u|^2_{\mathcal{H}_\delta^1}=\frac{2}{\pi}\int_{-\infty}^{\infty}I_\delta(\xi)\big|\mathscr{F}[u](\xi)\big|^2\,\mathrm{d}\xi,\quad I_\delta(\xi)=\int_0^{\delta}(1-\cos\xi s)\gamma_\delta(s)\,\mathrm{d}s. \tag{3.30}$$

We next estimate the bound of $I_\delta(\xi)$ with kernel function defined in (3.1). It is easy to show that for any $y\ge0$, we have $y^2/2-1+\cos y\ge0$. This implies

$$\frac{1-\cos\xi s}{s^2}\le\frac{\xi^2}{2},\quad s>0,\;\;\xi\in\mathbb{R}. \tag{3.31}$$

Hence, by (3.1), we have

$$I_\delta(\xi)\le\frac{\xi^2}{2}\int_0^{\delta}\omega_\delta(s)\,\mathrm{d}s\le C_\delta\frac{\xi^2}{2}\int_0^{\delta}s^{-\mu}\,\mathrm{d}s=\frac{C_\delta\delta^{1-\mu}}{2(1-\mu)}\xi^2. \tag{3.32}$$

Then by (3.30), (3.32) and Parseval's identity again,

$$\begin{aligned}|u|^2_{\mathcal{H}_\delta^1}&\le\frac{C_\delta\delta^{1-\mu}}{\pi(1-\mu)}\int_{-\infty}^{\infty}\xi^2\big|\mathscr{F}[u](\xi)\big|^2\,\mathrm{d}\xi=\frac{C_\delta\delta^{1-\mu}}{\pi(1-\mu)}\int_{-\infty}^{\infty}\mathrm{i}\xi\mathscr{F}[u](\xi)\cdot\overline{\mathrm{i}\xi\mathscr{F}[u](\xi)}\,\mathrm{d}\xi\\&=\frac{2C_\delta\delta^{1-\mu}}{1-\mu}\int_{-\infty}^{\infty}[u'(x)]^2\,\mathrm{d}x=\frac{2C_\delta\delta^{1-\mu}}{1-\mu}\|u'\|^2.\end{aligned} \tag{3.33}$$

This ends the proof. □

With the aid of Lemma 3.2, we can then properly choose $\varPsi$ in (3.23) to derive the error estimate of the orthogonal projection $\widehat{\varPi}_N^{\delta}$. We state the main result as follows.

Theorem 3.2. *Let $\gamma_\delta(s)$ be a general kernel function as in Lemma 3.2. If $\hat{\partial}_x^m u \in L^2(\mathbb{R})$ with $1 \le m \le N+1$, and $\hat{\partial}_x = \partial_x + x$, then we have the estimate*

$$\|u - \widehat{\Pi}_N^\delta u\|_{\mathcal{H}_\delta^1} \le c(D_{\delta,\mu}+1)N^{(1-m)/2}\|\hat{\partial}_x^m u\|, \tag{3.34}$$

where $D_{\delta,\mu}$ is the same as in (3.25)*, and c is a positive constant independent of N, δ and u.*

Proof. We have to resort to some intermediate orthogonal projections on approximation by Hermite functions. Let $\pi_N : L^2_\omega(\mathbb{R}) \to P_N$ be the L^2_ω-orthogonal projection, defined by

$$(u - \pi_N u, v_N)_\omega = 0, \quad \forall\, v_N \in P_N. \tag{3.35}$$

For any $u \in L^2(\mathbb{R})$, we have $u\mathrm{e}^{x^2/2} \in L^2_\omega(\mathbb{R})$. Define the operator

$$\widehat{\pi}_N u = \mathrm{e}^{-x^2/2}\pi_N(u\mathrm{e}^{x^2/2}) \in V_N. \tag{3.36}$$

By (3.35), it defines an L^2-orthogonal projection upon V_N, as

$$(u - \widehat{\pi}_N u, v_N) = (u\mathrm{e}^{x^2/2} - \pi_N(u\mathrm{e}^{x^2/2}), v_N\mathrm{e}^{x^2/2})_\omega = 0, \ \ \forall v_N \in V_N. \tag{3.37}$$

We refer to [18, Thm 7.14] for the estimates: *If $\hat{\partial}_x^m u \in L^2(\mathbb{R})$ with $l \le m \le N+1$ and $l = 0, 1$, then we have*

$$\|\partial_x^l(u - \widehat{\pi}_N u)\| \le cN^{(l-m)/2}\|\hat{\partial}_x^m u\|, \tag{3.38}$$

where c is a positive constant independent of N and u. With this, we derive from (3.23) and Lemma 3.2 immediately that

$$\|u - \widehat{\Pi}_N^\delta u\|_{\mathcal{H}_\delta^1} \le \|u - \widehat{\pi}_N u\|_{\mathcal{H}_\delta^1} \le (D_{\delta,\mu}+1)\|u - \widehat{\pi}_N u\|_{H^1} \le c(D_{\delta,\mu}+1)N^{(1-m)/2}\|\hat{\partial}_x^m u\|. \tag{3.39}$$

This ends the proof. □

Now, we are ready to estimate the error between the solutions of (3.5) and (3.7).

Theorem 3.3. *Let u and u_N be respectively the solutions of* (3.5) *and* (3.7) *with the kernel function $\gamma_\delta(s)$ given in Lemma 3.2. If $\hat{\partial}_x^m u \in L^2(\mathbb{R})$, $f \in C(\mathbb{R})$ and $\hat{\partial}_x^m f \in L^2(\mathbb{R})$ with $1 \le m \le N+1$, and $\hat{\partial}_x = \partial_x + x$, then for $\lambda > 0$, we have the estimate*

$$\|u - u_N\|_{\mathcal{H}_\delta^1} \le c\big((D_{\delta,\mu}+1)N^{(1-m)/2}\|\hat{\partial}_x^m u\| + N^{\frac{1}{6}-\frac{m}{2}}\|\hat{\partial}_x^m f\|\big), \tag{3.40}$$

where $D_{\delta,\mu}$ is the same as in (3.25)*, and c is a positive constant independent of N, δ, u and f.*

Proof. It follows from a standard procedure for error analysis under the Galerkin formulation. Here, we sketch the proof for completeness. By (3.5) and (3.7), we have

$$\mathbb{B}_\delta(u - u_N, \psi) = (f - \widehat{I}_N f, \psi), \quad \forall\, \psi \in V_N, \tag{3.41}$$

By the definition (3.21),

$$\begin{aligned}\mathbb{B}_\delta(\widehat{\Pi}_N^\delta u - u_N, \psi) &= \mathbb{B}_\delta(\widehat{\Pi}_N^\delta u - u, \psi) + (f - \widehat{I}_N f, \psi)\\ &= (\lambda-1)(\widehat{\Pi}_N^\delta u - u, \psi) + (f - \widehat{I}_N f, \psi), \quad \forall\, \psi \in V_N.\end{aligned} \tag{3.42}$$

Taking $\psi = \widehat{\Pi}_N^\delta u - u_N$ in the above, we infer from the Cauchy-Schwarz inequality that for $\lambda > 0$,

$$\begin{aligned}|\widehat{\Pi}_N^\delta u - u_N|^2_{\mathcal{H}_\delta^1} &+ \frac{\lambda}{2}\|\widehat{\Pi}_N^\delta u - u_N\|^2\\ &\le (\lambda-1)^2\lambda^{-1}\|\widehat{\Pi}_N^\delta u - u\|^2 + \lambda^{-1}\|f - \widehat{I}_N f\|^2.\end{aligned} \tag{3.43}$$

Recall the interpolation approximation result (see [18, Thm 7.18]): *For $f \in C(\mathbb{R})$ and $\hat{\partial}_x^m f \in L^2(\mathbb{R})$ with fixed $m \ge 1$, we have*

$$\|\widehat{I}_N f - f\| \le cN^{\frac{1}{6}-\frac{m}{2}}\|\hat{\partial}_x^m f\|, \tag{3.44}$$

where c is a positive constant independent of N and f. Using the triangle inequality, we will obtain the final result (3.40). □

4. Numerical results and discussions

4.1. **Test of accuracy.** We first consider the nonlocal diffusion model (1.5), and choose

$$\omega_\delta(s) = \frac{2-2\beta}{\delta^{2-2\beta}} s^{1-2\beta}, \quad \frac{1}{2} \le \beta < 1 \tag{4.1}$$

in (3.24) such that $\gamma_\delta(s) = \frac{2-2\beta}{\delta^{2-2\beta}} s^{-1-2\beta}$ has a normalised second moment. We test the scheme on three examples.

Example 4.1. $u(x) = \mathrm{e}^{-x^2}(2+\sin x)$ (exponential decay with oscillation at infinity).

We set $\lambda = 1$ in (1.5). Besides, we suppose $\delta = 0.1$ for nonlocal interaction and $\beta = 0.8$ in the kernel function $\gamma_\delta(s)$. The scaling factor in the basis are chosen in two different ways, as fixed values or adaptive values depending on the polynomial degree N.

To illustrate the rate of convergence, we depict in the left part of Figure 4.1 the discrete L^∞-errors obtained by 150 Hermite-Gauss points and the H^1_δ-errors with the scaling factor $\alpha = 1.4$. It indicates that these errors behave like e^{-cN}, where c is a constant independent of N. As the exact solution is smooth and decays exponentially, the observed convergence behaviour agrees with the theoretic result in Theorem 3.3.

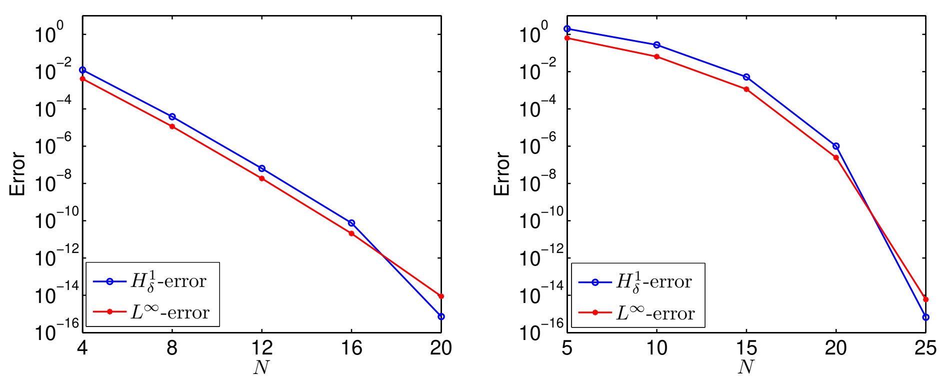

Figure 4.1: L^∞-errors and H^1_δ-errors against N in semi-log scale. Left: fixed α; Right: adaptive α_N.

To enhance the resolution of the approximation, we choose the scaling factor α depending on N (denoted by α_N). For a given accuracy threshold ϵ, we set

$$\alpha_N = x_N^{(N)}/M, \qquad M = \inf_y \{y : |u(x)| \le \epsilon, \ x \ge y\}, \tag{4.2}$$

where $x_N^{(N)}$ is the largest zero of the Hermite polynomial H_{N+1}. We use $\epsilon = 2\times 10^{-9}$. To illustrate the rate of convergence, we depict in Figure 4.1 (right) the L^∞-errors and the H^1_δ-errors. The graph demonstrates that the approximation has a super-geometric convergence rate for slightly large N. It turns out that the use of adaptive α_N can lift the convergence rate to super-geometric.

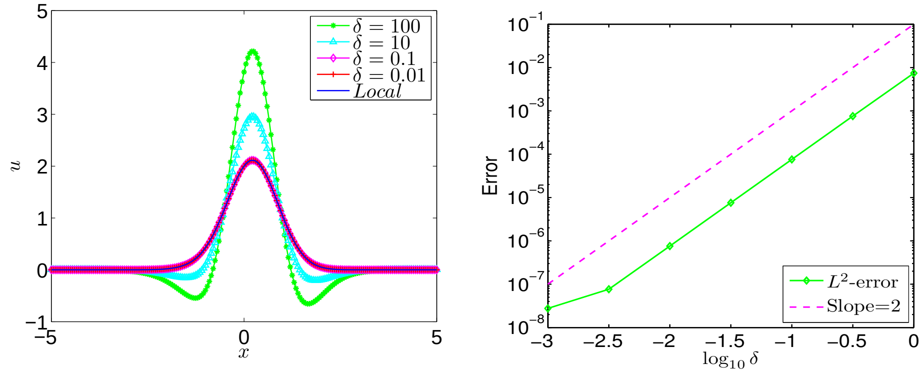

Figure 4.2: Left: Numerical solutions of nonlocal and local models; Right: L^2-errors against δ in log-log scale.

Letting δ approach zero, we investigate the approximation behaviour of nonlocal model (1.5) to its local counterpart, that is,

$$-u''(x) + \lambda u(x) = f(x), \quad x \in \mathbb{R}; \quad \lim_{|x|\to\infty} u(x) = 0. \tag{4.3}$$

For $u(x) = \mathrm{e}^{-x^2}(2 + \sin x)$ and $\lambda = 1$, we have

$$f(x) = \mathrm{e}^{-x^2}[2(3 - 4x^2) + 4(1 - x^2)\sin x + 4x\cos x]. \tag{4.4}$$

In (1.5), we choose $\delta = 100,\ 10,\ 0.1,\ 0.01$. In Figure 4.2 (left), we plot the four different nonlocal numerical solutions together with the local solution. It indicates that as δ becomes smaller, the nonlocal numerical solution approach the corresponding local one. This demonstrates our scheme is δ-robust/compatible. Here, we also intend to have some insights into the rate in δ when the numerical approximation of u_δ approaches that of u. For clarity, we denote the nonlocal numerical solution by u_N^δ and the local one by u_N^0, respectively. In Figure 4.2 (right), we plot the difference $u_N^\delta - u_N^0$ in L^2-norm against δ, and observe the convergence order $\mathcal{O}(\delta^2)$.

Example 4.2. $u(x) = \frac{1}{(1+x^2)^h}$ (algebraic decay without oscillation at infinity).

We take $\lambda = 2$, $\delta = 0.1$ and $\beta = 0.8$ in the model problem (1.5) with (4.1). We adopt the adaptive scaling factor as in (4.2) for two cases: (i) $h = 3$ and $\epsilon = 10^{-7}$; and (ii) $h = 4$ and $\epsilon = 10^{-8}$. We plot the H_δ^1-errors and L^∞-errors in Figure 4.3 (left) and it has a higher convergence rate than any algebraic order. In contrast, if one chooses a fixed α independent of N, one can only expect an algebraic order of convergence according to Theorem 3.3. In fact, it verifies that

$$\lim_{x\to\infty} \frac{|\hat{\partial}_x^m u(x)|}{\frac{|x|^m}{(1+x^2)^h}} = 1,$$

which means $\|\hat{\partial}_x^m u\| < \infty$ if and only if $m < 2h - \frac{1}{2}$, and the $\mathcal{H}_\delta^1$-errors will decay in $\mathcal{O}(N^{3/4-h})$ for sufficiently large N. According [18, Remark 7.5], the Hermite approximation with adaptive scaling factors has a convergence order higher than $\mathcal{O}(N^{3/4-h})$. For comparison, we also plot two reference lines in the same figure with the dotted line for the slope of $-\frac{9}{4}$, and the dashed line for the slope of $-\frac{13}{4}$.

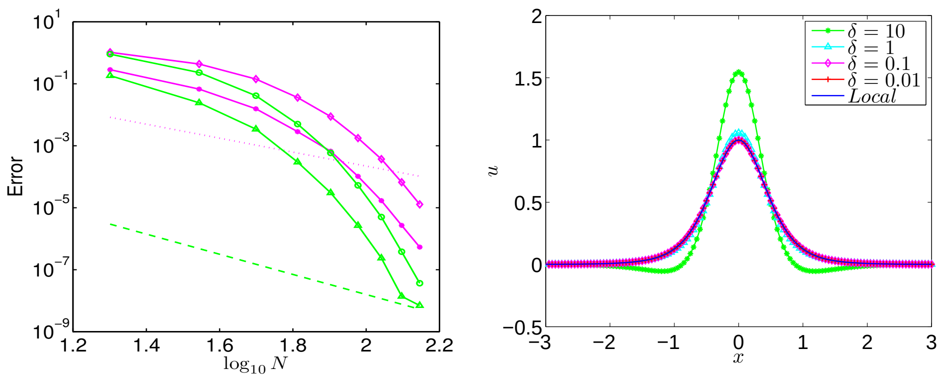

Figure 4.3: Left: L^∞-errors (• for $h = 3$ and △ for $h = 4$) and H^1_δ-errors (◇ for $h = 3$ and ○ for $h = 4$) against N in log-log scale; Right: numerical solutions of nonlocal and local models. The dotted line with the slope $-\frac{9}{4}$ and the dashed line with the slope $-\frac{13}{4}$ are used on the left side for reference.

As with the previous example, we take

$$f(x) = \frac{2}{(1+x^2)^h} + \frac{2h}{(1+x^2)^{h+1}} - \frac{4h(h+1)x^2}{(1+x^2)^{h+2}} \tag{4.5}$$

in (1.5) and (4.3). When $h = 3$, we calculate the numerical solutions of (1.5) for $\delta = 10,\ 1,\ 0.1,\ 0.01$ and those of (4.3), as plotted in Figure 4.3 (right). It is seen again that the nonlocal solutions tend to the local one as δ approaches zero.

Example 4.3. $u(x) = \frac{\sin kx}{(1+x^2)^h}$ (algebraic decay with oscillation at infinity).

We take $\lambda = 3,\ \delta = 0.1, \beta = 0.8$ and $k = 3$, and consider two cases: $h = 3$ and $h = 4$ with $\epsilon = 10^{-9}$ and $\epsilon = 10^{-11}$ for the adaptive scaling factor α_N, respectively. Then the H^1_δ-errors and L^∞-errors are plotted in Figure 4.4 (left). Similar to the previous example, higher convergence rates than any algebraic order are observed, although Theorem 3.3 predicts only an algebraic order in $\mathcal{O}(N^{3/4-h})$. Meanwhile the accuracy is inferior to the previous one due to the oscillatory factor $\sin kx$.

To explore the behaviour of the nonlocal solutions with different δ, we fix

$$f(x) = \frac{(k^2+3)\sin kx}{(1+x^2)^h} + \frac{2hkx\cos kx}{(1+x^2)^{h+1}} + \frac{2h\sin kx + 2hkx\cos kx}{(1+x^2)^{h+1}} - \frac{4h(h+1)x^2\sin kx}{(1+x^2)^{h+2}} \tag{4.6}$$

in (1.5) and (4.3). When $k = 3, h = 4$, we compute the numerical solution of (1.5) for $\delta = 5,\ 1,\ 0.1,\ 0.01$ and the solution of (4.3), and plot them in Figure 4.4 (right). When $\delta = 0.01$, the nonlocal solution almost overlaps the local one as the local solution is the limit of the nonlocal solution for $\delta \to 0$.

4.2. **Application to (truncated) fractional Laplacian.** For $\boldsymbol{s} \in \mathbb{R}^d$, we choose

$$\omega_\delta(\boldsymbol{s}) = C_{d,\gamma}|\boldsymbol{s}|^{2-d-\gamma} \quad \text{with} \quad C_{d,\gamma} = \frac{\gamma 2^{\gamma-1}\Gamma((\gamma+d)/2)}{\pi^{d/2}\Gamma((2-\gamma)/2)}, \quad \gamma \in [1,2) \tag{4.7}$$

in (3.24). According to the definition (1.4), we have

$$\mathcal{L}_\delta u(\boldsymbol{x}) = -C_{d,\gamma}\int_{|\boldsymbol{x}-\boldsymbol{y}|\le\delta} \frac{u(\boldsymbol{x}) - u(\boldsymbol{y})}{|\boldsymbol{x}-\boldsymbol{y}|^{d+\gamma}}\mathrm{d}\boldsymbol{y}, \quad \boldsymbol{x} \in \mathbb{R}^d. \tag{4.8}$$

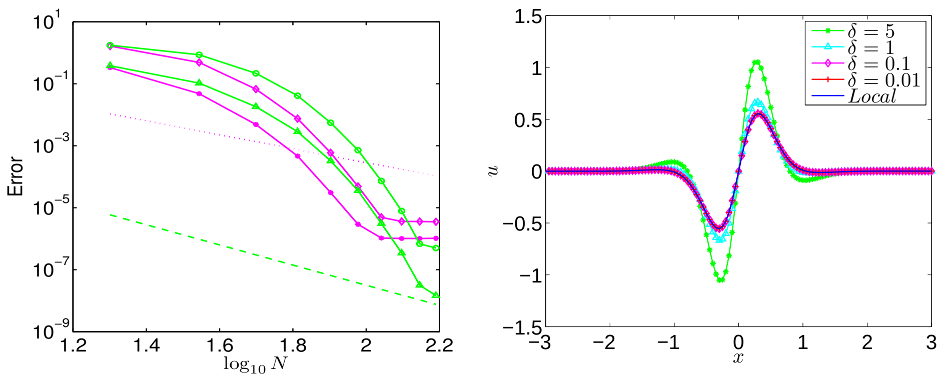

Figure 4.4: Left: L^∞-errors (• for $h = 3$ and △ for $h = 4$) and H^1_δ-errors (◇ for $h = 3$ and ○ for $h = 4$) against N in log-log scale; Right: numerical solutions of nonlocal and local models. The dotted line with the slope $-\frac{9}{4}$ and the dashed line with the slope $-\frac{13}{4}$ are used on the left side for reference.

Note that the nonlocal operator in (4.8) truncates the integration domain of the classical fractional Laplace operator from $\mathbb{R}^d$ to the δ-neighborhood of $\boldsymbol{x}$. Here we denote

$$(-\Delta_\delta)^{\gamma/2} u(\boldsymbol{x}) := -\mathcal{L}_\delta u(\boldsymbol{x}). \tag{4.9}$$

In what follows, we shall consider model problems containing one or more truncated fractional Laplace operators in one dimension. We adopt some examples as in [27].

Example 4.4. Consider the following fractional equation:

$$(-\Delta_\delta)^{\gamma/2} u(x) + 2u(x) = f(x), \quad x \in \mathbb{R}; \quad \lim_{|x|\to\infty} u(x) = 0. \tag{4.10}$$

Let $\delta = 0.1$, $\gamma = 1.4$, and the exact solution be $u(x) = \mathrm{e}^{-x^2/2} x^2 \cos(x/2)$. We present the numerical errors against the polynomial degree N in Figure 4.5. The scaling parameter is taken to be $\alpha = 0.9$. The results in Figure 4.5 (right) shows the exponential decay of the errors as expected.

For comparison purpose, we consider the fractional model with the usual integral fractional Laplacian:

$$(-\Delta)^{\gamma/2} u(x) + 2u(x) = f(x), \quad x \in \mathbb{R}; \quad \lim_{|x|\to\infty} u(x) = 0, \tag{4.11}$$

where $(-\Delta)^{\gamma/2} = (-\Delta_\infty)^{\gamma/2}$. In the test, we take $\delta = 0.01,\ 0.1,\ 0.5,\ 5$. From Figure 4.5 (right), we observe that when δ becomes larger, the difference between the nonlocal solution and the usual one becomes smaller. When $\delta = 5$, the nonlocal solution almost overlaps its usual counterpart.

Example 4.5. Consider the multi-term equation:

$$\sum_{j=1}^{J} (-\Delta_\delta)^{\gamma_j/2} u(x) = f(x), \quad x \in \mathbb{R}; \quad \lim_{|x|\to\infty} u(x) = 0. \tag{4.12}$$

Here we set $J = 4$, $\delta = 0.1$, $\gamma_1 = \sqrt{6} - \sqrt{2}$, $\gamma_2 = \sqrt{2}$, $\gamma_3 = 3 - \sqrt{2}$, $\gamma_4 = \sqrt{3}$ and the exact solution $u(x) = \mathrm{e}^{-2x^2/5}(\sin x + x^6 + x^2 \cos x)$. We choose $\alpha = 0.8$. The numerical errors in L^∞-norm against the polynomial degree N are plotted in Figure 4.6 (left). Exponential convergence is observed.

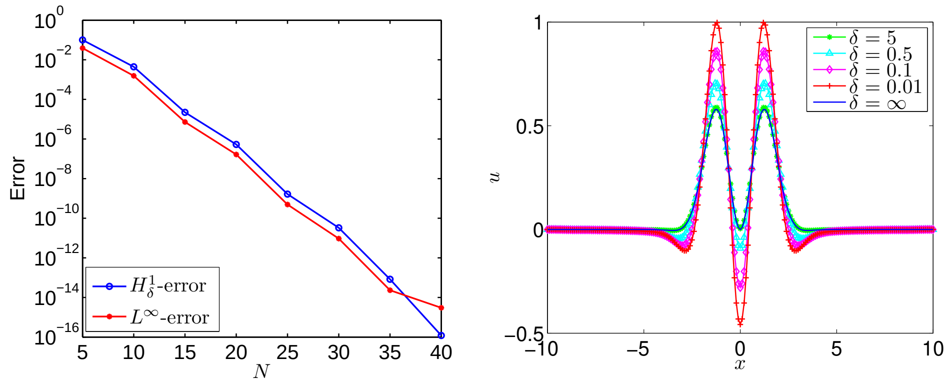

Figure 4.5: Left: L^∞-errors and H^1_δ-errors against N in semi-log scale; Right: numerical solutions of truncated and usual models.

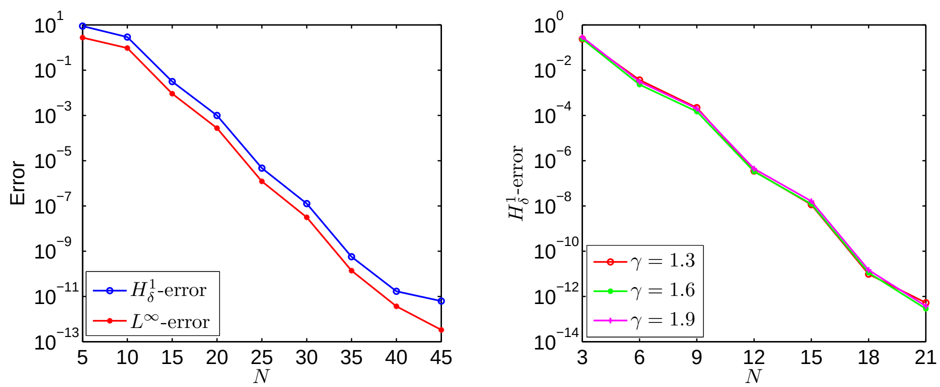

Figure 4.6: Left: L^∞-errors and H^1_δ-errors against N in semi-log scale (Example 4.5); Right: H^1_δ-errors against N in semi-log scale (Example 4.6).

Example 4.6. Consider the following nonlinear nonlocal model:

$$(-\Delta_\delta)^{\gamma/2} u(x) + u^2(x) = f(x), \quad x \in \mathbb{R}; \quad \lim_{|x|\to\infty} u(x) = 0. \tag{4.13}$$

The exact solution is chosen as $u(x) = \mathrm{e}^{-x^2/2}(\sin x + x^2)$. To deal with the nonlinear term $u^2(x)$, we use the Newton iteration method with a tolerance 10^{-14}. We set $\delta = 0.1$ and $\gamma = 1.3, 1.6, 1.9$. The approximation results are then depicted in Figure 4.6 (right), which shows the exponential convergence as predicted.

4.3. **Application to nonlocal Allen-Cahn equations.** We apply the solver for spatial discretisation of the nonlocal Allen-Cahn equation on the real line:

$$\begin{cases} \partial_t u(x,t) - \varepsilon^2 \mathscr{L}_\delta u(x,t) + u^3(x,t) - u(x,t) = 0, \;\; (x,t) \in \mathbb{R} \times (0,T], \\ \lim\limits_{|x| \to +\infty} u(x,t) = 0, \;\; t \in [0,T], \\ u(x,0) = u_0(x), \;\; x \in \mathbb{R}, \end{cases} \tag{4.14}$$

where the singular kernel function of the nonlocal operator $\mathscr{L}_\delta u(x,t)$ satisfies (4.1). Let $t_m = m\Delta t$, $m = 0,1,...,K$ with the time stepping size $\Delta t = \frac{T}{K}$, and let u^m be the approximation of $u(x,t)$ at time t_m. Then a second-order linearized implicit scheme in time is

$$\frac{u^{m+1} - u^m}{\Delta t} - \varepsilon^2 \mathscr{L}_\delta u^{m+1} + (u^m)^2 u^{m+1} - u^{m+1} = 0. \tag{4.15}$$

The full-discretised scheme is to find $u_N^{m+1} \in \mathcal{V}_N$, such that for all $v_N \in \mathcal{V}_N$,

$$\Big(\frac{1}{\Delta t} - 1\Big)(u_N^{m+1}, v_N) - \varepsilon^2 (\mathscr{L}_\delta u_N^{m+1}, v_N) + ((u_N^m)^2 u_N^{m+1}, v_N) = \frac{1}{\Delta t}(u_N^m, v_N). \tag{4.16}$$

We aim to numerically study the dynamics of the time-dependent equation and the influence of δ on the behaviour of solutions. We fix $\varepsilon = 0.1$ and choose $\Delta t = 0.001$ as the time step and $\beta = 0.8$ in the kernel. Besides, we put suitable scaling factor into the basis to improve the efficiency.

Example 4.7. Consider (4.14) with the initial value: $u_0(x) = \mathrm{e}^{-x^2/2}(\cos x + 2\sin 2x)$. As before, we make a comparison between the local and nonlocal solutions. Here we take $N = 128$ in the nonlocal model and $N = 64$ in the local model.

We plot the numerical solutions at different T against x in Figure 4.7, and observe that solutions under nonlocal setting with small δ are close to the local ones, while for large δ, they have visible differences. In Figure 4.8, we depict the solutions (with $\delta = 0.1$ for the nonlocal one) in $x \in [-5,5]$ and $t \in [0,10]$ in mesh and contour plots.

5. Hermite spectral-Galerkin methods in two dimensions

In this section, we extend the previous Hermite spectral-Galerkin method to the two-dimensional case. Consider the model equation:

$$-\mathcal{L}_\delta u(\boldsymbol{x}) + \lambda u(\boldsymbol{x}) = f(\boldsymbol{x}), \quad \boldsymbol{x} \in \mathbb{R}^2; \quad \lim_{|\boldsymbol{x}| \to \infty} u(\boldsymbol{x}) = 0, \tag{5.1}$$

where $\boldsymbol{x} = (x_1, x_2)$ and the kernel $\gamma_\delta(\boldsymbol{s})$ in the nonlocal operator is given by (4.7) with $d = 2$.

Define the energy space

$$\mathcal{H}_\delta^1(\mathbb{R}^2) := \Big\{ u \in L^2(\mathbb{R}^2) \,:\, \int_{\mathbb{R}^2} \int_{|\boldsymbol{s}| \le \delta} \big| u(\boldsymbol{x} + \boldsymbol{s}) - u(\boldsymbol{x}) \big|^2 \gamma_\delta(|\boldsymbol{s}|)\, \mathrm{d}\boldsymbol{s}\mathrm{d}\boldsymbol{x} < \infty \Big\}. \tag{5.2}$$

The weak formulation of (5.1) is to find $u \in H_\delta^1(\mathbb{R}^2)$ such that

$$\mathbb{B}_\delta(u,v) = (f,v), \quad \forall v \in H_\delta^1(\mathbb{R}^2), \tag{5.3}$$

where

$$\begin{aligned} \mathbb{B}_\delta(u,v) :=& \frac{1}{2} \int_{\mathbb{R}^2} \int_{|\boldsymbol{s}| \le \delta} (u(\boldsymbol{x}+\boldsymbol{s}) - u(\boldsymbol{x}))(\bar{v}(\boldsymbol{x}+\boldsymbol{s}) - \bar{v}(\boldsymbol{x})) \gamma_\delta(|\boldsymbol{s}|) \mathrm{d}\boldsymbol{s}\mathrm{d}\boldsymbol{x} \\ &+ \lambda \int_{\mathbb{R}^2} u(\boldsymbol{x}) \bar{v}(\boldsymbol{x}) \mathrm{d}\boldsymbol{x}. \end{aligned} \tag{5.4}$$

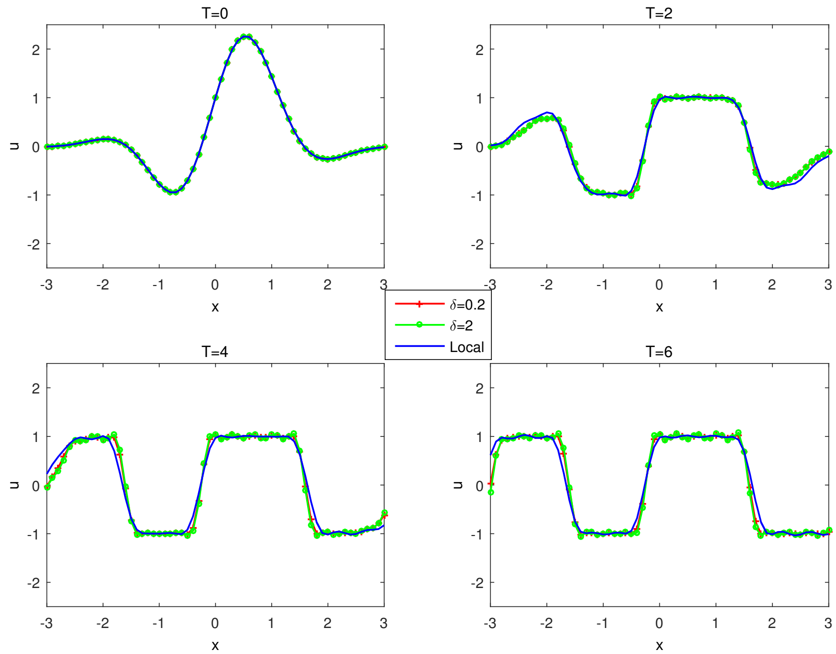

Figure 4.7: Snapshots of numerical solutions for both local and nonlocal Allen-Cahn equations at different time with $\delta = 2, 0.2$.

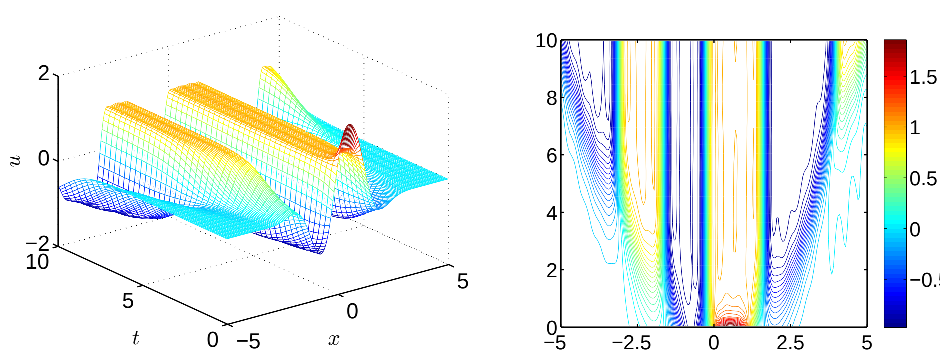

Figure 4.8: Time evolutions of the nonlocal numerical solution for $\delta = 0.1$. Left: the mesh plot; Right: the contour.

Note that the domain of $\boldsymbol{s}$ in the integral (5.4) is a disk with radius $\delta > 0$. It is natural to use polar coordinates $(r\cos\theta, r\sin\theta)$ for $\boldsymbol{s}$. We introduce the isotropic Hermite functions (cf. [23])

$$H_k^n(\boldsymbol{x}) = \mathcal{L}_k^n(|\boldsymbol{x}|^2)Y^n(\boldsymbol{x})\mathrm{e}^{-\frac{|\boldsymbol{x}|^2}{2}}, \quad n \in \mathbb{Z},\ k \geq n^-, \tag{5.5}$$

where $\mathcal{L}_k^n$ is the generalized Laguerre polynomial defined in (2.18), and $Y^n(\boldsymbol{x})$ is the normalized spherical harmonic function given by

$$Y^n(\boldsymbol{x}) = \frac{(x_1 + \mathrm{i}\, x_2)^n}{\sqrt{2\pi}} = \frac{r^n \mathrm{e}^{\mathrm{i}n\theta}}{\sqrt{2\pi}}, \quad n \in \mathbb{Z}. \tag{5.6}$$

Making use of the polar coordinates $\boldsymbol{x} = (x_1, x_2) = (r\cos\theta, r\sin\theta)$, the orthogonality relation of complex exponential functions, and the orthogonality relation (2.22) of the generalized Laguerre functions, we derive the following orthogonality relation of the isotropic Hermite functions,

$$\begin{aligned}\int_{\mathbb{R}^2} H_k^n(\boldsymbol{x})\overline{H_j^m}(\boldsymbol{x})\,\mathrm{d}\boldsymbol{x} &= \frac{1}{2\pi}\int_0^\infty \mathcal{L}_k^n(r^2)\mathcal{L}_j^m(r^2)\mathrm{e}^{-r^2} r^{n+m+1}\mathrm{d}r \int_0^{2\pi} \mathrm{e}^{\mathrm{i}(n-m)\theta}\mathrm{d}\theta \\ &= \frac{1}{2}\delta_{n,m}\int_0^\infty \mathcal{L}_k^n(\eta)\mathcal{L}_j^m(\eta)\mathrm{e}^{-\eta}\eta^{\frac{n+m}{2}}\,\mathrm{d}\eta = \frac{(k+n)!}{2\,k!}\delta_{k,j}\,\delta_{n,m}, \\ & n,m \in \mathbb{Z},\ k \ge n^-,\ j \ge m^-.\end{aligned} \tag{5.7}$$

Further, we define the orthonormal Hermite functions as

$$\widehat{H}_k^n(\boldsymbol{x}) = \sqrt{\frac{2k!}{(k+n)!}}H_k^n(\boldsymbol{x}) = \sqrt{\frac{k!}{\pi(k+n)!}}\mathcal{L}_k^n(r^2)r^n\mathrm{e}^{\mathrm{i}n\theta}\mathrm{e}^{-\frac{r^2}{2}},\ n\in\mathbb{Z},\ k\ge n^-. \tag{5.8}$$

The Hermite spectral-Galerkin scheme for (5.3) is to find

$$u_K^N \in \mathcal{V}_K^N := \mathrm{span}\big\{\widehat{H}_k^n\ :\ n^- \le k \le n^- + K,\ |n| \le N\big\}, \tag{5.9}$$

such that

$$\mathbb{B}_\delta(u_K^N, \psi) = (f, \psi), \quad \forall\, \psi \in \mathcal{V}_K^N, \tag{5.10}$$

For fixed $\delta > 0$, both (5.3) and (5.10) admit a unique solution, in view of the Lax-Milgram Lemma.

5.1. **Implementation.** The linear system of (5.10) takes the following equivalent form

$$(\boldsymbol{S} + \lambda\boldsymbol{M})\boldsymbol{u} = \boldsymbol{F}, \tag{5.11}$$

where

$$\boldsymbol{M} = (\boldsymbol{M}_{j,k}^{m,n})_{\substack{n^-\le k\le n^-+K,\ |n|\le N\\ m^-\le j\le m^-+K,\ |m|\le N}}, \qquad \boldsymbol{M}_{j,k}^{m,n} = (H_k^n, H_j^m) = \delta_{m,n}\delta_{j,k}, \tag{5.12}$$

$$\boldsymbol{S} = (\boldsymbol{S}_{j,k}^{m,n})_{\substack{n^-\le k\le n^-+K,\ |n|\le N\\ m^-\le j\le m^-+K,\ |m|\le N}}, \qquad \boldsymbol{S}_{j,k}^{m,n} = \mathbb{B}_\delta(H_k^n, H_j^m) = \frac{1}{2}\int_{|\boldsymbol{s}|\le\delta} \varPhi_{j,k}^{m,n}(\boldsymbol{s})\gamma_\delta(|\boldsymbol{s}|)\mathrm{d}\boldsymbol{s}, \tag{5.13}$$

and

$$\varPhi_{j,k}^{m,n}(\boldsymbol{s}) = 2\int_{\mathbb{R}^2}\widehat{H}_k^n(\boldsymbol{x})\overline{\widehat{H}_j^m}(\boldsymbol{x})\mathrm{d}\boldsymbol{x} - \int_{\mathbb{R}^2}\widehat{H}_k^n(\boldsymbol{x}+\boldsymbol{s})\overline{\widehat{H}_j^m}(\boldsymbol{x})\mathrm{d}\boldsymbol{x} - \int_{\mathbb{R}^2}\widehat{H}_k^n(\boldsymbol{x})\overline{\widehat{H}_j^m}(\boldsymbol{x}+\boldsymbol{s})\mathrm{d}\boldsymbol{x}. \tag{5.14}$$

The following result indicates the coefficient matrix of the linear system (5.11) is real symmetric and block-diagonal.

Theorem 5.1. *$\boldsymbol{S}$ is a real symmetric matrix with $\boldsymbol{S}_{j,k}^{m,n} = 0$ for $m \ne n$. For $k \ge n^-$ and $j \ge 2$, $\boldsymbol{S}_{j+k,k}^{n,n} = \boldsymbol{S}_{k,k+j}^{n,n}$ can be evaluated through the following recurrence relations*

$$\begin{aligned} S_{j+k,k}^{n,n} &= \frac{\sqrt{(k+1)(k+1+n)}}{\sqrt{(j+k)(j+k+n)}}S_{j+k-1,k+1}^{n,n} - \frac{2(j-1)}{\sqrt{(j+k)(j+k+n)}}S_{j+k-1,k}^{n,n} \\ &\quad + \frac{\sqrt{k(k+n)}}{\sqrt{(j+k)(j+k+n)}}S_{j+k-1,k-1}^{n,n} - \frac{\sqrt{(j+k-1)(j+k-1+n)}}{\sqrt{(j+k)(j+k+n)}}S_{j+k-2,k}^{n,n}, \\ &\qquad k = n^-, n^-+1, \ldots, \quad j = 2, 3, \ldots, \end{aligned} \tag{5.15}$$

with the initial conditions,

$$\boldsymbol{S}^{n,n}_{k,k} = 8\pi \int_0^{\frac{\delta}{2}} \Big[1 - \mathcal{L}^0_k(\eta^2)\mathcal{L}^0_{k+n}(\eta^2)\mathrm{e}^{-\eta^2}\Big]\eta\gamma_\delta(2\eta)\mathrm{d}\eta, \quad k = n^-, n^- + 1, \dots,$$
$$\boldsymbol{S}^{n,n}_{k+1,k} = \frac{8\pi}{\sqrt{(k+1+n)(k+1)}} \int_0^{\frac{\delta}{2}} \mathcal{L}^1_k(\eta^2)\mathcal{L}^1_{k+n}(\eta^2)\mathrm{e}^{-\eta^2}\eta^3\gamma_\delta(2\eta)\mathrm{d}\eta \quad k = n^-, n^- + 1, \dots. \tag{5.16}$$

5.2. **Proof of Theorem 5.1.** We need the following two lemmas to prove Theorem 5.1.

Lemma 5.1. *The isotropic Hermite functions are the eigenfunctions of the Fourier transform. More precisely,*

$$\mathscr{F}[\widehat{H}^n_k](\boldsymbol{\xi}) = 2\pi(-\mathrm{i})^{n+2k}\widehat{H}^n_k(\boldsymbol{\xi}). \tag{5.17}$$

Proof. Using polar coordinates $\boldsymbol{x} = (x_1, x_2) = (r\cos\theta, r\sin\theta)$ and $\boldsymbol{\xi} = (\xi_1, \xi_2) = (\rho\cos\phi, \rho\sin\phi)$, we derive that

$$\mathscr{F}\big[H^n_k\big](\boldsymbol{\xi}) = \int_{\mathbb{R}^2} H^n_k(\boldsymbol{x})\mathrm{e}^{-\mathrm{i}\boldsymbol{\xi}\cdot\boldsymbol{x}}\mathrm{d}x = \frac{1}{\sqrt{2\pi}}\int_0^\infty \mathcal{L}^n_k(r^2)\mathrm{e}^{-\frac{r^2}{2}}r^{n+1}\mathrm{d}r \int_0^{2\pi} \mathrm{e}^{-\mathrm{i}\rho r\cos(\theta-\phi)}\mathrm{e}^{in\theta}\mathrm{d}\theta.$$

Next, making change of coordinates $\theta \leftarrow \theta + \phi - \frac{\pi}{2}$, we further get from [33, (2.2.5)] that

$$\int_0^{2\pi} \mathrm{e}^{-\mathrm{i}\rho r\cos(\theta-\phi)}\mathrm{e}^{\mathrm{i}n\theta}\mathrm{d}\theta = \mathrm{e}^{\mathrm{i}n(\phi-\frac{\pi}{2})}\int_0^{2\pi} \mathrm{e}^{-\mathrm{i}\rho r\sin\theta}\mathrm{e}^{\mathrm{i}n\theta}\mathrm{d}\theta = 2\pi(-\mathrm{i})^n J_n(\rho r)\mathrm{e}^{\mathrm{i}n\phi}, \tag{5.18}$$

where J_n is the Bessel function of order n. As a result,

$$\begin{aligned}
\mathscr{F}[H^n_k](\boldsymbol{\xi}) &= \sqrt{2\pi}\,(-\mathrm{i})^n\,\mathrm{e}^{\mathrm{i}n\phi}\int_0^\infty \mathcal{L}^n_k(r^2)\mathrm{e}^{-\frac{r^2}{2}}r^{n+1}J_n(\rho r)\mathrm{d}r \\
&= \sqrt{2\pi}\,(-\mathrm{i})^n\,\rho^{-\frac{1}{2}}\,\mathrm{e}^{\mathrm{i}n\phi}\int_0^\infty \mathcal{L}^n_k(r^2)\mathrm{e}^{-\frac{r^2}{2}}r^{n+\frac{1}{2}}J_n(\rho r)(\rho r)^{\frac{1}{2}}\mathrm{d}r \\
&= \sqrt{2\pi}\,(-\mathrm{i})^n\,\rho^{-\frac{1}{2}}\,\mathrm{e}^{\mathrm{i}n\phi}\,(-1)^k\mathcal{L}^n_k(\rho^2)\mathrm{e}^{-\frac{\rho^2}{2}}\rho^{n+\frac{1}{2}} \\
&= 2\pi\,(-\mathrm{i})^{n+2k}H^n_k(\boldsymbol{\xi}),
\end{aligned}$$

where we have used an identity on the Hankel transform of the Bessel function in [13, P. 42] for the second equality sign. By (5.8), we now verify the conclusion. □

Next we present the convolution formula of isotropic Hermite functions.

Lemma 5.2. *We have the convolution property*

$$[\widehat{H}^n_k * \widehat{H}^m_j](\boldsymbol{x}) = \int_{\mathbb{R}^2} \widehat{H}^n_k(\boldsymbol{s}-\boldsymbol{x})\widehat{H}^m_j(\boldsymbol{x})\mathrm{d}\boldsymbol{x} = \pi\widehat{H}^{m-k+j}_k\big(\frac{\boldsymbol{x}}{2}\big)\widehat{H}^{n-j+k}_j\big(\frac{\boldsymbol{x}}{2}\big). \tag{5.19}$$

Proof. By (5.17) we have

$$\begin{aligned}
\mathscr{F}[H^n_k * H^m_j](\boldsymbol{\xi}) &= \mathscr{F}[H^n_k](\boldsymbol{\xi})\cdot\mathscr{F}[H^m_j](\boldsymbol{\xi}) = (2\pi)^2\,(-\mathrm{i})^{n+m+2k+2j}H^n_k(\boldsymbol{\xi})H^m_j(\boldsymbol{\xi}) \\
&= (2\pi)^2\,(-\mathrm{i})^{n+m+2k+2j}\mathcal{L}^n_k(|\boldsymbol{\xi}|^2)\mathcal{L}^m_j(|\boldsymbol{\xi}|^2)Y^n(\boldsymbol{\xi})Y^m(\boldsymbol{\xi})\mathrm{e}^{-|\boldsymbol{\xi}|^2}.
\end{aligned}$$

Using polar coordinates $\boldsymbol{x} = (r\cos\theta, r\sin\theta)$ and $\boldsymbol{\xi} = (\rho\cos\phi, \rho\sin\phi)$, we further get

$$\begin{aligned}
&[H^n_k * H^m_j](\boldsymbol{x}) = \frac{1}{4\pi^2}\int_{\mathbb{R}^2} \mathscr{F}[H^n_k * H^m_j](\boldsymbol{\xi})\,\mathrm{e}^{\mathrm{i}\boldsymbol{\xi}\cdot\boldsymbol{x}}\mathrm{d}\boldsymbol{\xi} \\
&= \frac{(-\mathrm{i})^{n+m+2k+2j}}{2\pi}\int_0^\infty \mathcal{L}^n_k(\rho^2)\mathcal{L}^m_j(\rho^2)\mathrm{e}^{-\rho^2}\rho^{m+n+1}\mathrm{d}\rho\int_0^{2\pi} \mathrm{e}^{\mathrm{i}(n+m)\phi}\,\mathrm{e}^{\mathrm{i}\rho r\cos(\phi-\theta)}\mathrm{d}\phi.
\end{aligned}$$

Making change of variable $\phi \leftarrow \phi + \pi$ yields

$$\int_0^{2\pi} \mathrm{e}^{\mathrm{i}(n+m)\phi}\, \mathrm{e}^{\mathrm{i}\rho r\cos(\phi-\theta)} \mathrm{d}\phi = (-1)^{n+m} \int_0^{2\pi} \mathrm{e}^{\mathrm{i}(n+m)\phi}\, \mathrm{e}^{-\mathrm{i}\rho r\cos(\phi-\theta)} \mathrm{d}\phi \overset{(5.18)}{=} 2\pi\, \mathrm{i}^{m+n} J_{m+n}(\rho r) \mathrm{e}^{\mathrm{i}(m+n)\theta}.$$

Resorting the following integral identity for $y > 0, \Re\alpha > 0, \Re\nu > -1$ [19, (5)],

$$\int_0^\infty \rho^{\nu+1} \mathrm{e}^{-\alpha\rho^2} \mathcal{L}_j^{\nu-\sigma}(\alpha\rho^2) \mathcal{L}_k^{\sigma}(\alpha\rho^2) J_\nu(\rho r) \mathrm{d}\rho = \frac{(-1)^{j+k}}{2\alpha}\Big(\frac{r}{2\alpha}\Big)^{\nu} \mathrm{e}^{-\frac{r^2}{4\alpha}} \mathcal{L}_j^{\sigma-j+k}\Big(\frac{r^2}{4\alpha}\Big) \mathcal{L}_k^{\nu-\sigma+j-k}\Big(\frac{r^2}{4\alpha}\Big),$$

we finally derive that

$$\begin{aligned}
[H_k^n * H_j^m](\boldsymbol{x}) &= (-1)^{k+j}\, \mathrm{e}^{\mathrm{i}(m+n)\theta} \int_0^\infty \mathcal{L}_k^n(\rho^2) \mathcal{L}_j^m(\rho^2) \mathrm{e}^{-\rho^2} \rho^{m+n+1} J_{m+n}(\rho r)\, \mathrm{d}\rho \\
&= \frac{1}{2}\, \mathrm{e}^{\mathrm{i}(m+n)\theta} \Big(\frac{r}{2}\Big)^{m+n} \mathrm{e}^{-\frac{r^2}{4}} \mathcal{L}_k^{m-k+j}\Big(\frac{r^2}{4}\Big) \mathcal{L}_j^{n-j+k}\Big(\frac{r^2}{4}\Big) \\
&= \pi H_k^{m-k+j}\Big(\frac{\boldsymbol{x}}{2}\Big) H_j^{n-j+k}\Big(\frac{\boldsymbol{x}}{2}\Big),
\end{aligned}$$

which together with (5.8) gives (5.19). This completes the proof. □

We now return to the proof of Theorem 5.1. Noting that

$$\begin{aligned}
\overline{\widehat{H}_k^n}(\boldsymbol{x}) &= \sqrt{\frac{k!}{\pi\,(k+n)!}} \mathcal{L}_k^n(|\boldsymbol{x}|^2)(x_1 - \mathrm{i}x_2)^n \mathrm{e}^{-\frac{|\boldsymbol{x}|^2}{2}} \\
&\overset{(2.23)}{=} \sqrt{\frac{(k+n)!}{\pi\, k!}} \mathcal{L}_{k+n}^{-n}(|\boldsymbol{x}|^2)(-|\boldsymbol{x}|^2)^{-n}(x_1 - \mathrm{i}x_2)^n \mathrm{e}^{-\frac{|\boldsymbol{x}|^2}{2}} \\
&= (-1)^n \sqrt{\frac{(k+n)!}{\pi\, k!}} \mathcal{L}_{k+n}^{-n}(|\boldsymbol{x}|^2)(x_1 + ix_2)^{-n} \mathrm{e}^{-\frac{|\boldsymbol{x}|^2}{2}} \\
&= (-1)^n \widehat{H}_{k+n}^{-n}(\boldsymbol{x}) = \widehat{H}_{k+n}^{-n}(-\boldsymbol{x}),
\end{aligned}$$

we get from (5.19) that

$$\begin{aligned}
&\varPhi_{j,k}^{m,n}(\boldsymbol{s}) = 2(\widehat{H}_k^n, \widehat{H}_j^m) - [\widehat{H}_k^n * \widehat{H}_{j+m}^{-m}](\boldsymbol{s}) - [\widehat{H}_k^n * \widehat{H}_{j+m}^{-m}](-\boldsymbol{s}) \\
&= 2\delta_{m,n}\delta_{j,k} - \pi \widehat{H}_k^{j-k}\Big(\frac{\boldsymbol{s}}{2}\Big) \widehat{H}_{j+m}^{n+k-j-m}\Big(\frac{\boldsymbol{s}}{2}\Big) - \pi \widehat{H}_k^{j-k}\Big(\frac{-\boldsymbol{s}}{2}\Big) \widehat{H}_{j+m}^{n+k-j-m}\Big(\frac{-\boldsymbol{s}}{2}\Big) \\
&= (1 + (-1)^{m+n}) \Big[\delta_{m,n}\delta_{j,k} - \pi \widehat{H}_k^{j-k}\Big(\frac{\boldsymbol{s}}{2}\Big) \widehat{H}_{j+m}^{n+k-j-m}\Big(\frac{\boldsymbol{s}}{2}\Big)\Big] \\
&= (1 + (-1)^{m+n}) \Big[\delta_{m,n}\delta_{j,k} - \sqrt{\frac{k!(j+m)!}{j!(k+n)!}} \mathcal{L}_k^{j-k}(\eta^2) \mathcal{L}_{j+m}^{n-m+k-j}(\eta^2) \mathrm{e}^{-\eta^2} (\eta \mathrm{e}^{\mathrm{i}\varpi})^{n-m}\Big],
\end{aligned}$$

where we have used the polar coordinates $\boldsymbol{s}=(2\eta\cos\varpi, 2\eta\sin\varpi)$ for the last equality sign. In the sequel, we derive that

$$\begin{aligned}\boldsymbol{S}_{j,k}^{m,n} &= \frac{1+(-1)^{m+n}}{2}\int_{|\boldsymbol{s}|\le\delta}\Big[\delta_{m,n}\delta_{j,k}-\pi\widehat{H}_k^{j-k}\Big(\frac{\boldsymbol{s}}{2}\Big)\overline{\widehat{H}_{j+m}^{n+k-j-m}\Big(\frac{\boldsymbol{s}}{2}\Big)}\Big]\gamma_\delta(|\boldsymbol{s}|)\mathrm{d}\boldsymbol{s}\\ &=2(1+(-1)^{m+n})\int_0^{2\pi}\mathrm{e}^{\mathrm{i}(n-m)\varpi}\mathrm{d}\varpi\\ &\quad\times\int_0^{\frac{\delta}{2}}\Big[\delta_{m,n}\delta_{j,k}-\sqrt{\frac{k!(j+m)!}{j!(k+n)!}}\mathcal{L}_k^{j-k}(\eta^2)\mathcal{L}_{j+m}^{n-m+k-j}(\eta^2)\mathrm{e}^{-\eta^2}\eta^{n-m}\Big]\eta\gamma_\delta(2\eta)\mathrm{d}\eta\\ &=8\pi\delta_{m,n}\int_0^{\frac{\delta}{2}}\Big[\delta_{j,k}-\sqrt{\frac{k!(j+n)!}{j!(k+n)!}}\mathcal{L}_k^{j-k}(\eta^2)\mathcal{L}_{j+n}^{k-j}(\eta^2)\mathrm{e}^{-\eta^2}\Big]\eta\gamma_\delta(2\eta)\mathrm{d}\eta.\end{aligned}\tag{5.20}$$

It is now easy to see that the Hermitian matrix $\boldsymbol{S}$ is real symmetric and $\boldsymbol{S}_{j,k}^{m,n}=0$ if $m\ne n$. Next, to obtain a recurrence relation for $\boldsymbol{S}_{j,k}^{n,n}$, we resort to the identities (2.19)-(2.21), then find that

$$\begin{aligned}&(k+1)\mathcal{L}_{k+1}^{j-k-1}(\zeta)\mathcal{L}_{j+n}^{k-j+1}(\zeta)-j\mathcal{L}_k^{j-k-1}(\zeta)\mathcal{L}_{j+n-1}^{k-j+1}(\zeta)\\ &\quad-(j+1+n)\mathcal{L}_k^{j-k+1}(\zeta)\mathcal{L}_{j+n+1}^{k-j-1}(\zeta)+(k+n)\mathcal{L}_{k-1}^{j-k+1}(\zeta)\mathcal{L}_{j+n}^{k-j-1}(\zeta)\\ &\overset{(2.20)}{=}\big[j\mathcal{L}_k^{j-k-1}(\zeta)-\zeta\mathcal{L}_k^{j-k}(\zeta)\big]\mathcal{L}_{j+n}^{k-j+1}(\zeta)-j\mathcal{L}_k^{j-k-1}(\zeta)\mathcal{L}_{j+n-1}^{k-j+1}(\zeta)\\ &\quad-\mathcal{L}_k^{j-k+1}(\zeta)\big[(k+n)\mathcal{L}_{j+n}^{k-j-1}(\zeta)-\zeta\mathcal{L}_{j+n}^{k-j}(\zeta)\big]+(k+n)\mathcal{L}_{k-1}^{j-k+1}(\zeta)\mathcal{L}_{j+n}^{k-j-1}(\zeta)\\ &=j\mathcal{L}_k^{j-k-1}(\zeta)\big[\mathcal{L}_{j+n}^{k-j+1}(\zeta)-\mathcal{L}_{j+n-1}^{k-j+1}(\zeta)\big]-\zeta\mathcal{L}_k^{j-k}\mathcal{L}_{j+n}^{k-j+1}(\zeta)\\ &\quad-(k+n)\big[\mathcal{L}_k^{j-k+1}(\zeta)-\mathcal{L}_{k-1}^{j-k+1}(\zeta)\big]\mathcal{L}_{j+n}^{k-j-1}(\zeta)+\zeta\mathcal{L}_k^{j-k+1}(\zeta)\mathcal{L}_{j+n}^{k-j}(\zeta)\\ &\overset{(2.19)}{=}\big[j\mathcal{L}_k^{j-k-1}(\zeta)+\zeta\mathcal{L}_k^{j-k+1}(\zeta)\big]\mathcal{L}_{j+n}^{k-j}(\zeta)-\mathcal{L}_k^{j-k}(\zeta)\big[(k+n)\mathcal{L}_{j+n}^{k-j-1}(\zeta)+\zeta\mathcal{L}_{j+n}^{k-j+1}(\zeta)\big]\\ &\underset{(2.20)}{\overset{(2.19)}{=}}\big[-j\mathcal{L}_{k-1}^{j-k}(\zeta)+(2j+1)\mathcal{L}_k^{j-k}(\zeta)-(k+1)\mathcal{L}_{k+1}^{j-k}(\zeta)\big]\mathcal{L}_{j+n}^{k-j}(\zeta)\\ &\quad-\mathcal{L}_k^{j-k}(\zeta)\big[-(k+n)\mathcal{L}_{j+n-1}^{k-j}(\zeta)+(2k+2n+1)\mathcal{L}_{j+n}^{k-j}(\zeta)-(j+n+1)\mathcal{L}_{j+n+1}^{k-j}(\zeta)\big]\\ &\overset{(2.21)}{=}(\zeta+j-k)\mathcal{L}_k^{j-k}(\zeta)\mathcal{L}_{j+n}^{k-j}(\zeta)-(\zeta+k-j)\mathcal{L}_k^{j-k}(\zeta)\mathcal{L}_{j+n}^{k-j}(\zeta)\\ &=2(j-k)\mathcal{L}_k^{j-k}(\zeta)\mathcal{L}_{j+n}^{k-j}(\zeta).\end{aligned}\tag{5.21}$$

Let us temporarily define

$$\Phi_{j,k}^n(\zeta):=\delta_{j,k}-\sqrt{\frac{k!(j+n)!}{j!(k+n)!}}\mathcal{L}_k^{j-k}(\zeta)\mathcal{L}_{j+n}^{k-j}(\zeta)\mathrm{e}^{-\zeta}.$$

We further derive from (5.21) that

$$\begin{aligned}&\sqrt{(k+1)(k+1+n)}\Phi_{j,k+1}^n(\zeta)+\sqrt{k(k+n)}\Phi_{j,k-1}^n(\zeta)-\sqrt{(j+1)(j+1+n)}\Phi_{j+1,k}^n(\zeta)\\ &\qquad-\sqrt{j(j+n)}\Phi_{j-1,k}^n(\zeta)+2(k-j)\Phi_{j,k}^n(\zeta)=0,\end{aligned}$$

which yields (5.15).

As for the initial values, we declare from (5.20) that

$$\begin{aligned}\boldsymbol{S}_{k,k}^{n,n}&=8\pi\int_0^{\frac{\delta}{2}}\Big[1-\mathcal{L}_k^0(\eta^2)\mathcal{L}_{k+n}^0(\eta^2)\mathrm{e}^{-\eta^2}\Big]\eta\gamma_\delta(2\eta)\,\mathrm{d}\eta,\quad k\ge n^-,\\ \boldsymbol{S}_{k+1,k}^{n,n}&=-8\pi\sqrt{\frac{k+1+n}{k+1}}\int_0^{\frac{\delta}{2}}\mathcal{L}_k^1(\eta^2)\mathcal{L}_{k+1+n}^{-1}(\eta^2)\mathrm{e}^{-\eta^2}\eta\gamma_\delta(2\eta)\mathrm{d}\eta,\end{aligned}$$

$$\overset{(2.23)}{=} \frac{8\pi}{\sqrt{(k+1+n)(k+1)}} \int_0^{\frac{\delta}{2}} \mathcal{L}_k^1(\eta^2)\mathcal{L}_{k+n}^1(\eta^2)\mathrm{e}^{-\eta^2}\eta^3\gamma_\delta(2\eta)\mathrm{d}\eta \quad k \geq n^{-},$$

which gives (5.16). Now the proof is complete.

5.3. **Numerical results.** We take $\delta = 0.1$ and $\gamma = 1.4$, and test for two exact solutions $u(x) = \mathrm{e}^{-(x_1^2+x_2^2)/2}(1 - x_1^2/10)^4(1 + x_1^2/10)^6$ and $u(x) = \mathrm{e}^{-(x_1^2+x_2^2)/2}\sin(x_1x_2)$. In Figure 5.1, we plot the errors between the numerical results and the exact solutions in maximum norm against the polynomial degree N. We observe the spectral convergence in both cases as in one dimension shown in the previous section.

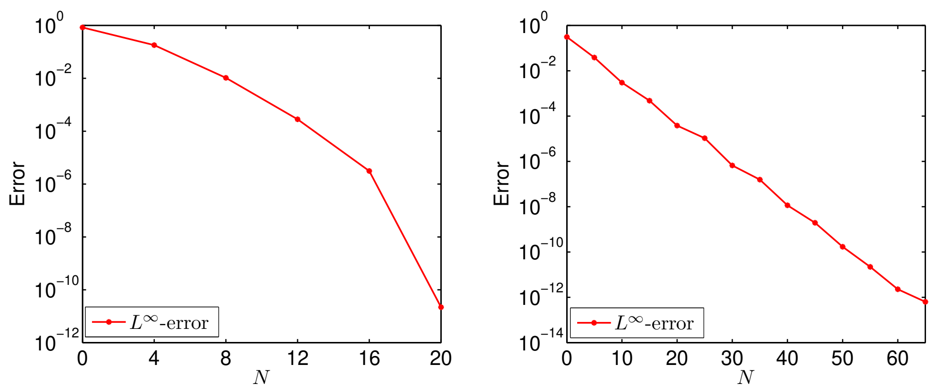

Figure 5.1: L^∞-errors against N in semi-log scale. Left: $u(x) = \mathrm{e}^{-(x_1^2+x_2^2)/2}(1 - x_1^2/10)^4(1 + x_1^2/10)^6$; Right: $u(x) = \mathrm{e}^{-(x_1^2+x_2^2)/2}\sin(x_1x_2)$.

We remark that a common way to discretise (5.3) is based on the tensor product basis of Hermite functions (cf. [24, 27]). However, the computational cost of the stiffness matrix is $\mathcal{O}(N^6)$ and the coefficient matrix is full that the complexity of solving the linear system using Gauss elimination method is also $\mathcal{O}(N^6)$. In comparison, our method of isotropic Hermite functions has remarkable advantages in view of the recursive formula given in Theorem 5.1.

References

[1] B. Aksoylu and M. L. Parks. Variational theory and domain decomposition for nonlocal problems. *Appl. Math. Comput.*, 217(14):6498–6515, 2011.

[2] W. Bao, H. Li, and J. Shen. A generalized Laguerre-Fourier-Hermite pseudospectral method for computing the dynamics of rotating Bose-Einstein condensates. *SIAM J. Sci. Comput.*, 31(5):3685–3711, 2009.

[3] H. R. Beyer, B. Aksoylu, and F. Celiker. On a class of nonlocal wave equations from applications. *J. Math. Phys.*, 57(6):062902, 2016.

[4] M. Cozzi and T. Passalacqua. One-dimensional solutions of non-local Allen-Cahn-type equations with rough kernels. *J. Differ. Equ.*, 260(8):6638–6696, 2016.

[5] M. D'Elia and M. Gunzburger. The fractional Laplacian operator on bounded domains as a special case of the nonlocal diffusion operator. *Comput. Math. Appl.*, 66(7):1245–1260, 2013.

[6] M. D'Elia, Q. Du, C. Glusa, M. Gunzburger, X. Tian, and Z. Zhou, Numerical methods for nonlocal and fractional models, *Acta Numer.,* 29 (2020), pp. 1–124.

[7] Q. Du. *Nonlocal Modeling, Analysis, and Computation.* Society for Industrial and Applied Mathematics, Philadelphia, 2019.

[8] Q. Du, M. Gunzburger, R. B. Lehoucq, and K. Zhou. Analysis and approximation of nonlocal diffusion problems with volume constraints. *SIAM Review*, 54(4):667–696, 2012.

[9] Q. Du, M. Gunzburger, R. B. Lehoucq, and K. Zhou. A nonlocal vector calculus, nonlocal volume-constrained problems, and nonlocal balance laws. *Math. Models Methods Appl. Sci.*, 23(03):493–540, 2013.

[10] Q. Du, H. D. Han, J. W. Zhang, and C. X. Zheng. Numerical solution of a two-dimensional nonlocal wave equation on unbounded domains. *SIAM J. Sci. Comput.*, 40:A1430–A1445, 2018.

[11] Q. Du and J. Yang. Fast and accurate implementation of Fourier spectral approximations of nonlocal diffusion operators and its applications. *J. Comput. Phys.*, 332:118–134, 2017.

[12] Q. Du, J. W. Zhang, and C. X. Zheng. Nonlocal wave propagation in unbounded multi-scale media. *Commun. Comput. Phys.*, 24:1049–1072, 2018.

[13] A. Erdélyi, W. Magnus, F. Oberhettinger, and F. G. Tricomi. *Tables of Integral Transforms: Vol.2*. McGraw-Hill Book Company, Incorporated, 1954.

[14] M. Felsinger, M. Kassmann, and P. Voigt. The Dirichlet problem for nonlocal operators. *Mathematische Zeitschrift*, 279(3-4):779–809, 2015.

[15] F. W. J. Olver, D. W. Lozier, R. F. Boisvert, and C. W. Clark. *NIST Handbook of Mathematical Functions*. Cambridge University Press, New York, 2010.

[16] G. Szegö. *Orthogonal Polynomials, 4th Ed.* Amer. Math. Soc., Providence, RI, 1975.

[17] I. S. Gradshteyn and I. M. Ryzhik. *Table of Integrals, Series and Products*. Academic Press, New York, 8th edition edition, 2015.

[18] J. Shen, T. Tang, and L.-L. Wang. *Spectral Methods: Algorithms, Analysis and Applications*. Springer-Verlag, New York, 2011.

[19] K.S. Kolbig and H. Scherb. On a Hankel transform integral containing an exponential function and two Laguerre polynomials. *CERN/Computing and Networks Division*, 95(4), 1995.

[20] C. Lasser and S. Troppmann. Hagedorn wavepackets in time-frequency and phase space. *J. Fourier Anal. Appl.*, 20(4):679–714, 2014.

[21] F. J. Liu, H. Y. Li, and Z. Q. Wang. A fully diagonalized spectral method using generalized Laguerre functions on the half line. *Adv. Comput. Math.* , 43(6):1227–1259, 2017.

[22] M. Abramowitz and I. A. Stegun. *Handbook of Mathematical Functions with Formulas, Graphs and Mathematical Tables*. Dover, New York, 1972.

[23] S. N. Ma, H. Y. Li, and Z. Zhang. Novel spectral methods for Schördinger equations with an inverse square potential on the whole space. *Discrete Contin. Dyn. Syst. Ser. B,*, 24(4): 1589-1615, 2019.

[24] Z. P. Mao and J. Shen. Hermite spectral methods for fractional PDEs in unbounded domains. *SIAM J. Sci. Comput.*, 39(5):A1928–A1950, 2017.

[25] C. T. Sheng, J. Shen, T. Tang, L.-L. Wang, and H. Yuan, Fast Fourier-like mapped Chebyshev spectral-Galerkin methods for PDEs with integral fractional Laplacian in unbounded domains, *SIAM J. Numer. Anal.,* 58 (2020), pp. 2435–2464.

[26] C. T. Sheng, S. N. Ma, H. Y. Li, L.-L. Wang, and L. L. Jia. Generalised Hermite spectral methods for PDEs involving integral fractional Laplacian and Schrödinger operators. *ESAIM: Math. Model. Numer. Anal.*, In review, 2020.

[27] T. Tang, H. Yuan, and T. Zhou. Hermite spectral collocation methods for fractional PDEs in unbounded domains. *Commun. Comput. Phys.*, 24(4):1143–1168, 2018.

[28] T. Tang, L.-L. Wang, H. Yuan, and T. Zhou. Rational spectral methods for PDEs involving fractional Laplacian in unbounded domains. *SIAM J. Sci. Comput.,* Vol. 42, No. 42, A585-A611, 2020.

[29] Y. Z. Tao, X. C. Tian, and Q. Du. Nonlocal diffusion and peridynamic models with Neumann type constraints and their numerical approximations. *Appl. Math. Comput.*, 305:282–298, 2017.

[30] X. C. Tian and Q. Du. Analysis and comparison of different approximations to nonlocal diffusion and linear peridynamic equations. *SIAM J. Numer. Anal.*, 51(6):3458–3482, 2013.

[31] X. C. Tian and Q. Du. Asymptotically compatible schemes and applications to robust discretization of nonlocal models. *SIAM J. Numer. Anal.*, 52(4):1641–1665, 2014.

[32] X. C. Tian and Q. Du. Nonconforming discontinuous Galerkin methods for nonlocal variational problems. *SIAM J. Numer. Anal.*, 53(2):762–781, 2015.

[33] G. N. Watson *A Treatise on the Theory of Bessel Functions, 2nd Edition*. Cambridge University Press, Cambridge, 1944.

[34] A. Yurova. *Generalized anisotropic Hermite functions and their applications*. PhD thesis, Technische Universität München, 2020.

[35] W. Zhang, J. Yang, J. W. Zhang, and Q. Du. Artificial boundary conditions for nonlocal heat equations on unbounded domain. *Commun. Comput. Phys.*, 21:16–39, 2017.

[36] C. X. Zheng, J. S. Hu, Q. Du, and J. W. Zhang. Numerical solution of the nonlocal diffusion equation on the real line. *SIAM J. Sci. Comput.*, 39(5):A1951–A1968, 2017.